

Fig 1-25 (a) Construction of sella (S). (b) Structural superimposition demonstrates the shift of S during growth. Superimposition of successive Sella points is therefore unreliable. (Adapted from Björk and Skieller⁹⁷ with permission.)

Melsen¹⁰⁰ and Björk¹⁰¹ found that sella is not stable during growth because of the eccentric remodeling pattern of the fossa hypophyseos (Fig 1-25). In addition, these authors found that nasion and basion changed considerably in position, variably in direction, and in amount. Therefore, these landmarks are also unreliable references. This is extensively reviewed in chapter 2.

Several investigators compared Björk's method with other procedures. Again, controversy developed. Some workers based their recommendations primarily on statistical evaluation of accuracy without due recognition of the importance of the validity of reference structures. Others concluded that the differences were too small to be of significance for selecting a procedure. Still other investigators stressed that validity is the decisive aspect and demonstrated the consequences of that view.¹⁰²⁻¹⁰⁸ Often, even in recent clinical reports, the validity and reliability of the superimposition method used are unclear.

Arat et al¹⁰⁹ recently compared the validity of superimposition methods by Ricketts,^{40,41} Steiner,⁹⁰ and Björk and Skieller.^{56,79,97} They noted that the origin of the differences is the instability of the reference landmarks. Their conclusion was that the Steiner and Ricketts methods are invalid because they may result in erroneous interpretation of growth and treatment changes. Histologic studies^{48,49} proved that nearly all of the periosteal reference landmarks were subject to growth changes.

Reflecting on the history of superimposition, we must conclude that subjective methods have been proposed. They were gradually accepted and became used on the basis of convention and tradition. However, all these methods—except one, the structural method—are based on circumstantial reasoning without any evidence.

The importance of selecting an evidence-based superimposition method is demonstrated in Figs 1-26 to 1-35. Pretreatment and end-of-retention tracings of one normal growing orthodontic patient, with common intervals between the films, without an extreme growth pattern, and without spectacular changes were selected. Identical records were used to create three sets of superimpositions produced with three different superimposition methods:

- Cranial base superimpositions (see Figs 1-26 to 1-29): Steiner/Tweed, Ricketts, and Björk structural superimpositions are compared.
- Local mandibular superimpositions (see Figs 1-30 to 1-32): Best-fit, Ricketts, and Björk structural superimpositions are compared.
- Local maxillary superimpositions (see Figs 1-33 to 1-35): Best-fit, Ricketts, and Björk structural superimpositions are compared.

Figs 1-26 to 1-36 Three sets of superimpositions (cranial base, local mandibular, and local maxillary) created using three different methods. Four colors in two shades are used: cranial base region (*gray*); maxillary region (*green*); mandibular region (*blue*); soft tissue (*pink*). The nasion-ptyergomaxillary fissure (Na-PTM) line reflects the sutural and nasal septum attachment of the midfacial structures to the anterior cranial base (see also chapter 3 and Fig 3-10). Not also that the Björk structural superimposition is repeated in Figs 1-27 and 1-29 for ease of comparison with the Steiner/Tweed and Ricketts superimpositions. Figures 1-26 to 1-29 and 1-34 to 1-36 superimpose the pretreatment and end-of-retention tracings.

Fig 1-26 Cranial base superimposition according to the Steiner/Tweed model. Anterior cranial base superimposition is on the sella-nasion (S-Na) line, registered at S. Both landmarks are unstable during the pubertal growth period. The difference between the registration on S in the Steiner/Tweed superimposition and the Björk structural superimposition (see Fig 1-27) is rather small. However, the positional change of Na in the Steiner model is upward/forward, while in the structural model (see Fig 1-27), the movement is downward/forward. The end-of-retention tracing is rotated forward around S in the Steiner/Tweed superimposition. The roofs of the orbits appear to remodel upward, while the middle cranial base remodels downward and forward, so that the temporomandibular joints also come forward and downward. The nasal floor and palate show almost no downward angle, only frontal forward displacement, which reflects the rotation of the S-Na line. The mandible seems to be displaced forward and downward by two modes: downward and forward remodeling of the joint fossa and condylar growth. The mandibular line (tangent to the lower border) seems to become displaced in parallel, with very little change in inclination.

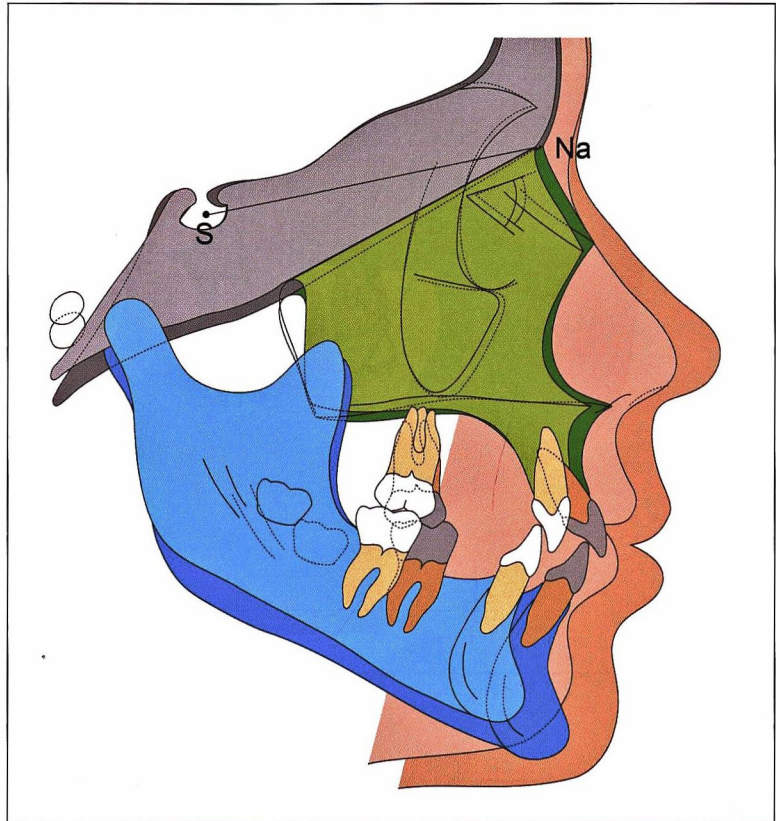
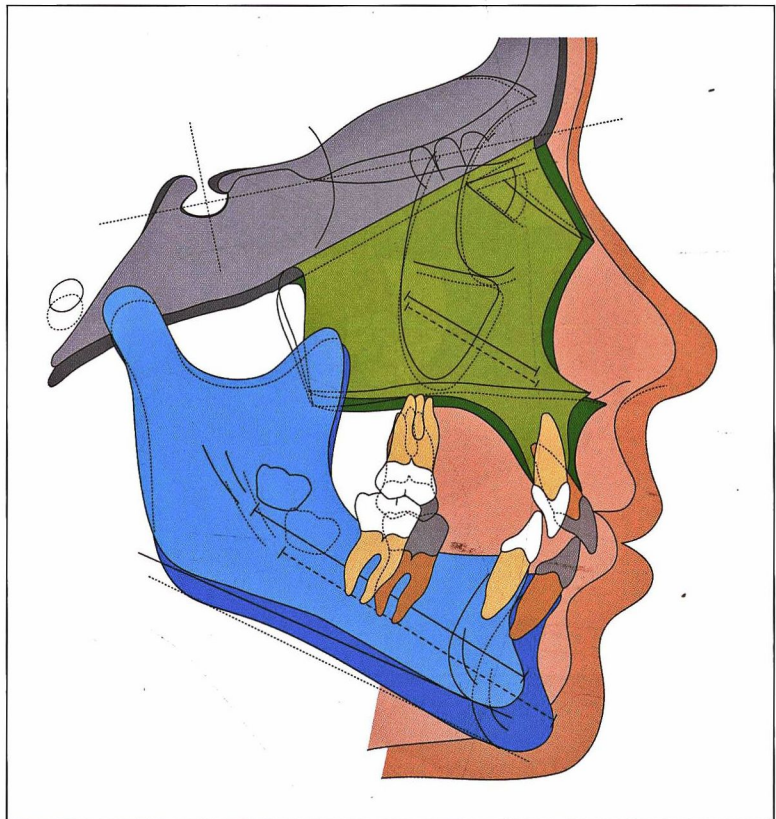


Fig 1-27 Cranial base superimposition according to the Björk structural model. All of the remodeling and displacement changes that are supposed to have occurred according to the Steiner/Tweed superimposition (see Fig 1-26) are shown to be considerably different in the structural superimposition because of the growth changes that have occurred at Na. Because of the superimposition on the S-Na line and registration at S in the Steiner/Tweed model, the differences in the cranial base are transferred to the posterior cranial base. The effect is a seemingly exaggerated downward remodeling of basion that results in the underestimation of vertical growth of the maxilla and the mandible in the Steiner/Tweed superimposition. An additional major difference results from the positional change of the fossa; mandibular condylar growth appears underestimated in the Steiner/Tweed model because of the downward movement of the joint. The structural superimposition reveals a slight posterior rotation of the mandibular line; a slight posterior "total rotation" has occurred. The Steiner/Tweed model seems to predict a more favorable treatment outcome with more forward mandibular growth and less vertical development. However, that outcome is not substantiated by the evidence-based structural method.



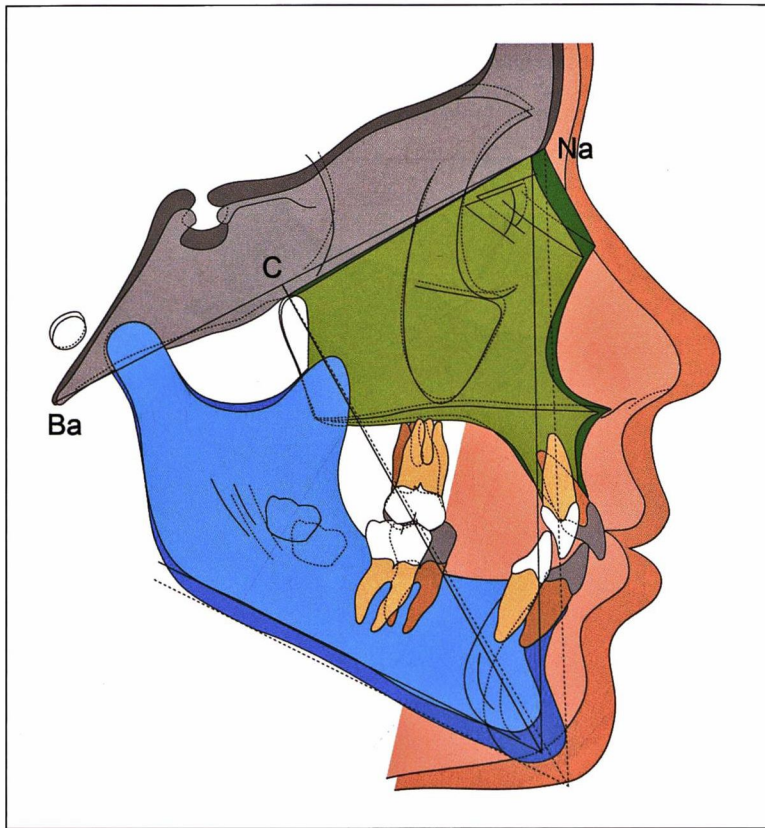


Fig 1-28 Cranial base superimposition according to the Ricketts model. For observation of overall changes, the Ricketts method uses the nasion-basion (Na-Ba) line to orient the tracings and registers on point C, the posterior upper limit of the pterygomaxillary fissure. The changes of sella and surrounding structures are very different when compared with the findings of the structural superimposition (see Fig 1-29). With the Ricketts model, the effect on the perceived growth of the facial structures is that the temporomandibular joint and mandible are underestimated and concealed, specifically the downward growth by the sutural system of the midface. This also may lead to the impression that the nasal floor does not descend by resorption, as is shown in the structural superimposition, but rather shows some deposition because it (along with the nasal spine) would move slightly upward. Enlow and Bang⁵⁴ demonstrated that such a remodeling pattern is highly unlikely and contrary to what has been found histologically.

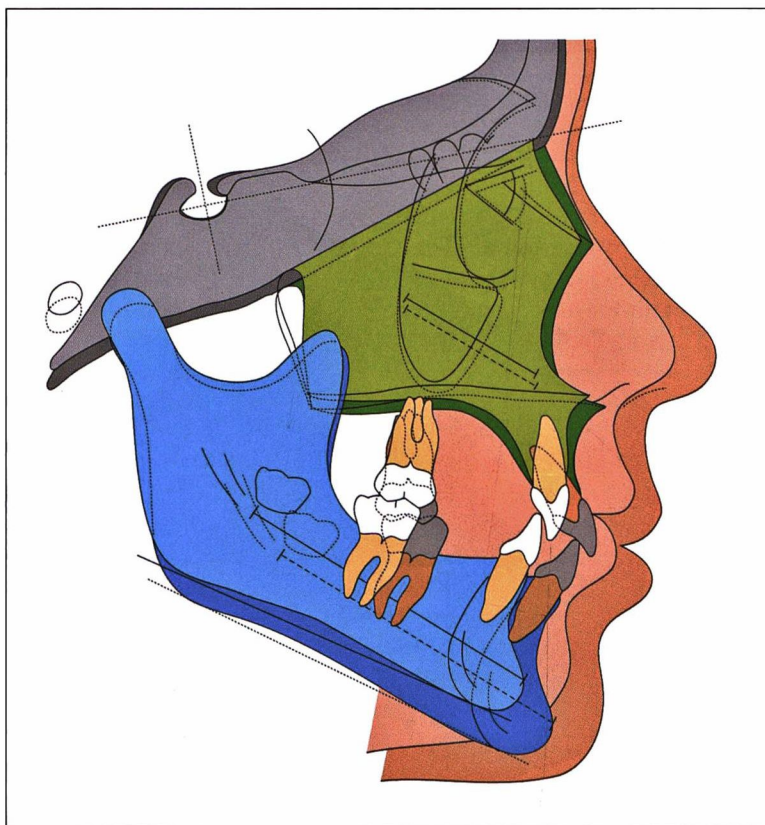


Fig 1-29 Cranial base superimposition according to the Björk structural model (same as Fig 1-27). The well-documented growth pattern^{95,100,101} of the midsagittal portion of the cranial base does not confirm the Ricketts superimposition. Nasion and basion change considerably in position, even during the relatively short time interval shown. The Ricketts procedure (see Fig 1-28) shows the mandibular lines as parallel and thus conceals the slight mandibular posterior total rotation that is revealed by the Björk structural method. The general impression of the Ricketts procedure is that it is rooted in conclusions preset from the start. Preconceived ideas of treatment effect are unconsciously confirmed by the selection of a particular type of superimposition.

Fig 1-30 Superimposition on the lower contour of the symphysis and the lower border of the body (corpus) of the mandible according to the best-fit model. The result is that the dorsal growth of the ramus is shown parallel to the original contour. The dorsal contours of the ascending ramus are parallel to each other.

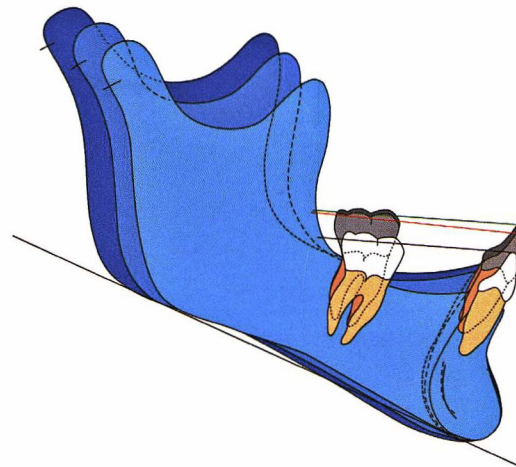


Fig 1-31 Mandibular superimposition according to the Björk structural model. The contours are not parallel, and the direction of condylar growth is much more vertical compared with that shown in the best-fit superimposition (see Fig 1-30) and in the Ricketts model (see Fig 1-32). The three techniques also differ in perceived movements of the first molar and mandibular anterior region. In the best-fit model, the molar shows backward and upward movement, while in the structural model, molar movement is only slightly backward and later forward again. In the Ricketts model, movement of the dentition is only vertical, not forward

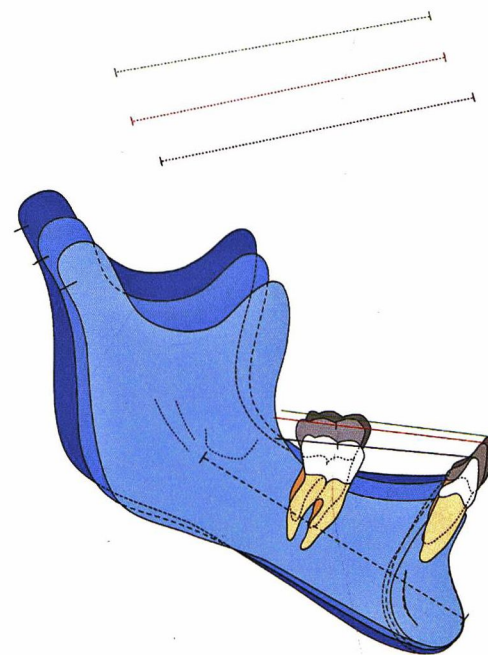
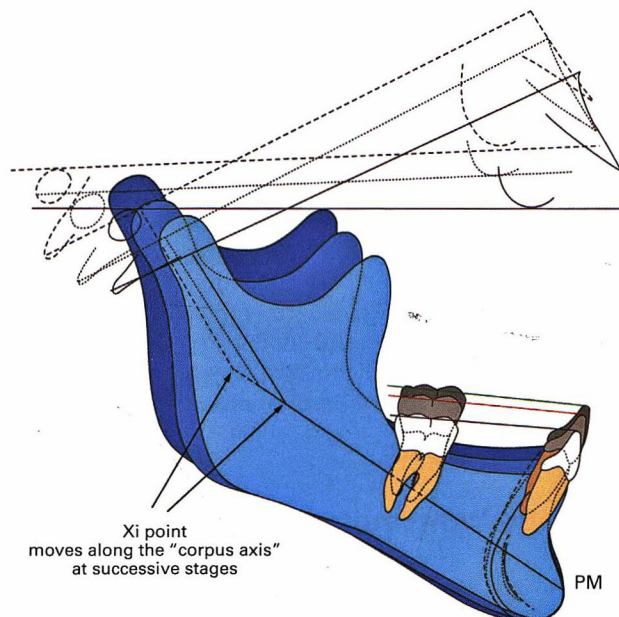


Fig 1-32 Mandibular superimposition according to the Ricketts model. Xi point is the center of the ramus and located halfway between the lowest point of the sigmoid notch and the point immediately inferior to it, on the lower border of the ramus in the Frankfort horizontal orientation and halfway on the minimum depth of the ramus. It was introduced by Ricketts but is not a stable point in the corpus¹¹⁰ (see chapter 2). In fact, Xi moves considerably upward during growth due to the remodeling of the reference points and lines used to construct Xi. The effect of this is clearly reflected in the perceived direction of condylar growth. Ricketts et al⁴¹ introduced the corpus axis, protuberance menti-Xi (PM-Xi) as an alternative for the traditional mandibular plane in superimpositions because of the remodeling in the gonial region found by Björk.^{26,58,79,101} PM is located at the symphysis at the crest of the mental protuberance at the point of recess of anterior contours.



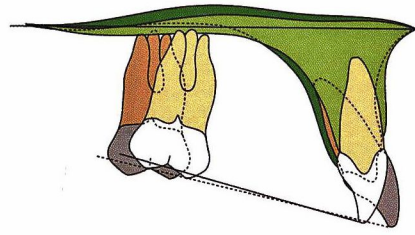


Fig 1-33 Maxillary superimposition according to the best-fit model. This superimposition masks the vertical remodeling of the maxilla shown in the structural superimposition (see Fig 1-34). Also note that the definition of anatomical fit for local maxillary superimposition is somewhat variable in the literature. Baumrind et al⁷⁸ define this as "the simple outline of the hard palate." This comes close to the definition used by Moorrees et al⁶¹: "the nasal floor, the apex of the palatal vault and any identifiable opaque detail in the trabecular area between the inner surface of the nasal floor, palatal vault and sub-nasal cortical plate, as well as any irregularity that can be identified on the outer and inner contours of the nasal floor and palate." Frequently, the line from the anterior nasal spine to the posterior nasal spine is used as an orientation. However, both landmarks are unstable.

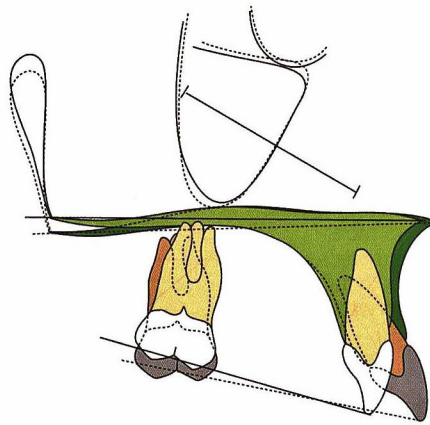


Fig 1-34 Maxillary superimposition according to the Björk structural model. The superimposition reveals some slight anterior rotation of the maxilla, which is masked in the best-fit model (see Fig 1-33). Remember that these tracings represent a treated patient, who showed considerable tooth movements.

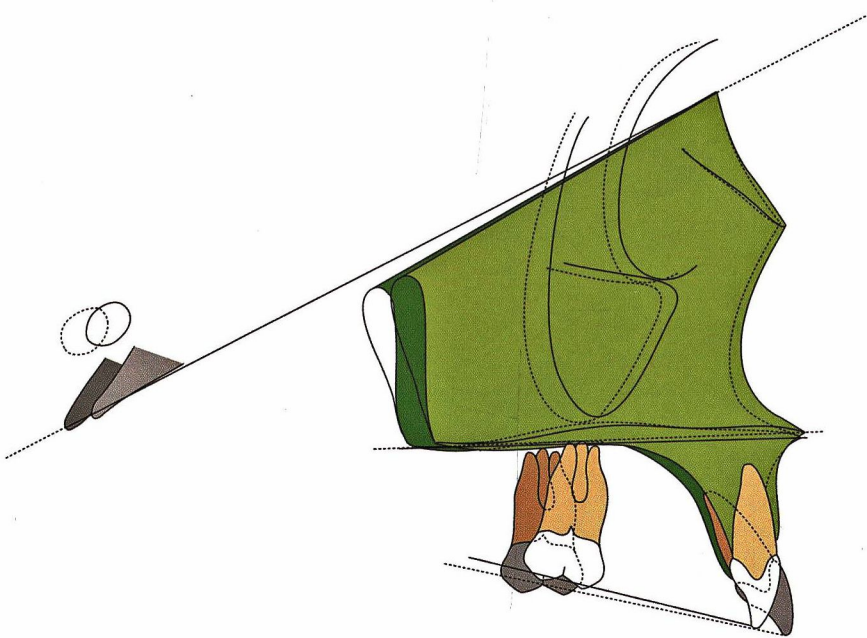


Fig 1-35 Maxillary superimposition according to the Ricketts model.⁴¹ This superimposition suggests considerable backward sutural displacement and only a little downward remodeling of the maxilla, with resorption at the front and considerable deposition at the bony palate. In the structural superimposition (see Fig 1-34), the first molar moves forward and downward, while in the Ricketts superimposition the first molar shows backward and downward movement. This suggests an overestimation of treatment effects in the Ricketts superimposition.

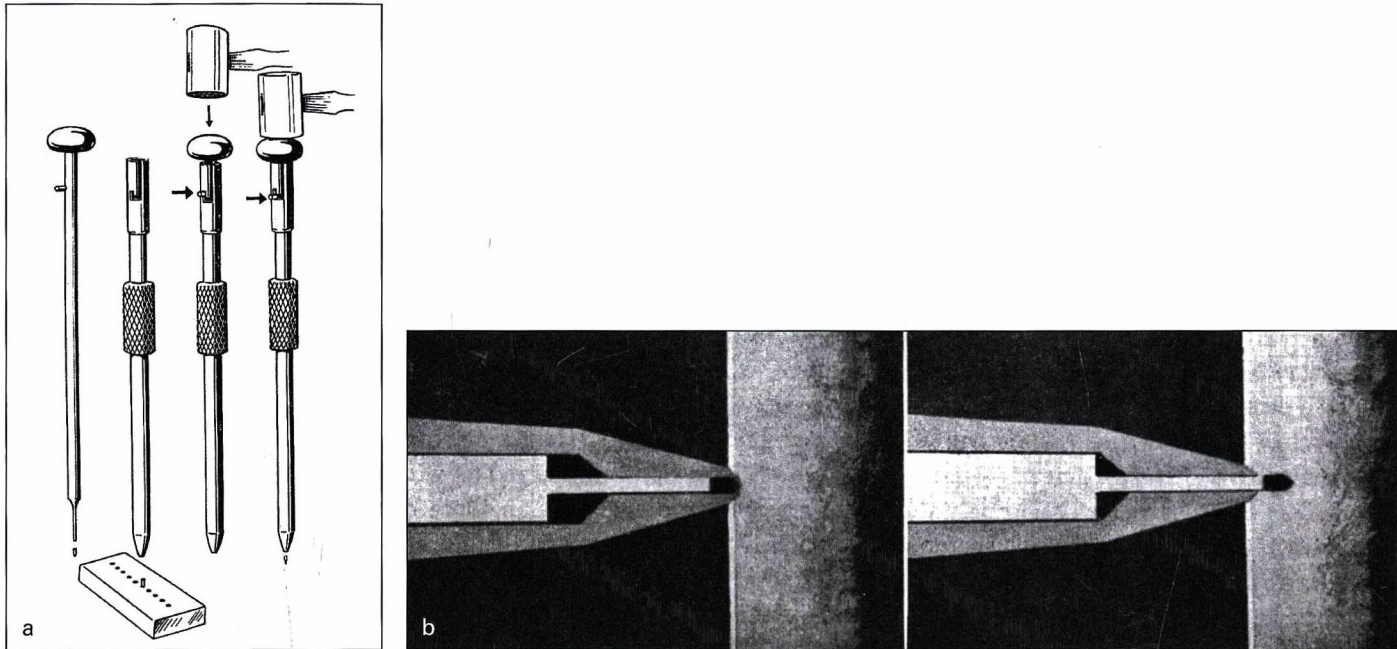
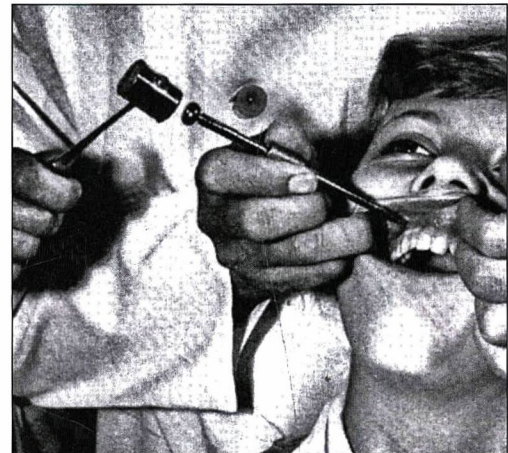


Fig 1-36 Metallic implants used as stable markers for facial growth evaluation. (a) Chrome-cobalt alloy pins (0.62-mm diameter; 2.00-mm length) were used initially; later, hardened tantalum pins (0.50-mm diameter; 1.50-mm length) that were more radiopaque (atomic number 73) and had better tissue compatibility were used. The instrument consists of a cylinder and piston, the point of which has the same diameter as the implants. A bayonet fitting limits the movement of the piston to the length of the implants. (Reprinted from Björk²⁶ with permission.) (b) For stability, the instrument is pressed against the bone (left). The implant is located a short distance from the tip of the instrument before it is hammered in place. In its final position, the piston projects beyond the tip of the instrument (right), so that the implant is driven deeper into the bone. (Reprinted from Björk⁵⁸ with permission.)

Fig 1-37 Placement of implant markers. A local anesthetic is applied to the sites where implants are to be placed. "The operator uses his or her left arm to steady the patient's head and his or her right hand to press the point of the instrument firmly against the bone. The instrument is grasped like a pencil and its sharp muzzle penetrates the periosteum. It enters a short distance into the bone, getting a firm purchase that prevents it from shifting while the pin is being driven into the bone and obviates any risk that the pin will not enter straight. The assistant drives home the implant with a smart tap of a lead mallet."²⁶ Three to four implants were inserted in each jaw. (Reprinted from Björk²⁶ with permission.)



Development of the Structural Method

History of the implant method

The structural method is the unparalleled achievement of Arne Björk, who developed it on the basis of his implant studies. During the period from 1951 to 1985, Björk studied facial growth longitudinally in more than 200 humans in whom metallic implants were placed as stable markers in selected positions in the jaws. By 1963, more than 900 implants had been placed in 110 children.⁵⁸

The first publication in which Björk²⁶ describes the clinical application of the implant method dates from 1955, and it is

a historic scientific breakthrough in the study of the human head (details of the technique were presented in later publications [Figs 1-36 to 1-38]). Five patients were described at 2-year intervals, and each had a different individual growth pattern (Fig 1-39).

In this first publication, Björk had not yet developed the sophisticated use of implant lines and the procedures to demonstrate growth rotations that characterize his later publications.

Evolution of the structural method

The placement of metallic implants into the deeper structures of the human head, such as the cranial base, was impossible. However, a fundamental histologic study of

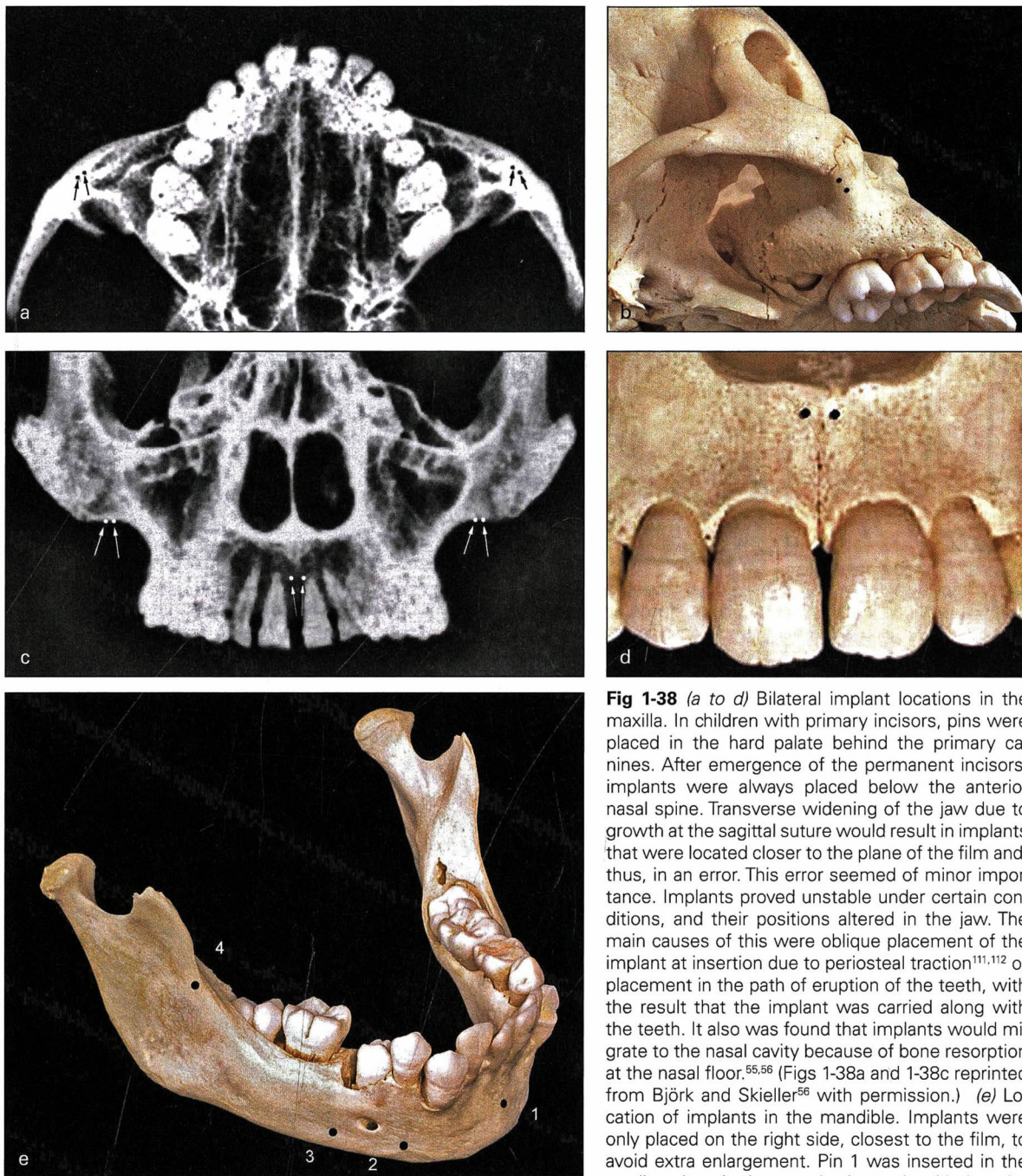


Fig 1-38 (a to d) Bilateral implant locations in the maxilla. In children with primary incisors, pins were placed in the hard palate behind the primary canines. After emergence of the permanent incisors, implants were always placed below the anterior nasal spine. Transverse widening of the jaw due to growth at the sagittal suture would result in implants that were located closer to the plane of the film and, thus, in an error. This error seemed of minor importance. Implants proved unstable under certain conditions, and their positions altered in the jaw. The main causes of this were oblique placement of the implant at insertion due to periosteal traction^{111,112} or placement in the path of eruption of the teeth, with the result that the implant was carried along with the teeth. It also was found that implants would migrate to the nasal cavity because of bone resorption at the nasal floor.^{55,56} (Figs 1-38a and 1-38c reprinted from Björk and Skieller⁵⁶ with permission.) (e) Location of implants in the mandible. Implants were only placed on the right side, closest to the film, to avoid extra enlargement. Pin 1 was inserted in the median plane in the symphysis at a level below the apices of the incisor. Pins 2 and 3 were placed below the first and second premolars, respectively. Pin 4 was placed on the external aspect of the ramus, level with the occlusal surface of the molars. This pin sometimes was gradually exposed due to resorption and a new one was needed. (Adapted from Björk with permission.⁵⁸)

human autopsy material of the cranial base in growing individuals by Birte Melsen,¹⁰⁰ University of Århus, Denmark, complemented and refined the anterior cranial base superimposition proposed by Björk.¹⁰¹

On the basis of the evidence produced by Melsen and Björk, it became possible to identify those structures in the cranial base that are stable after a certain age on cephalometric radiographs.

The investigations of the cranial base and the implant studies of the maxilla and the mandible resulted in funda-

mental progress in two aspects: (1) demonstration of individual variation of growth patterns and (2) identification of natural reference markers.

Demonstration of individual variation of growth patterns

The implant cases demonstrated the large individual variation of growth patterns of the dentofacial complex. This resulted in new and unparalleled understanding of how variations in

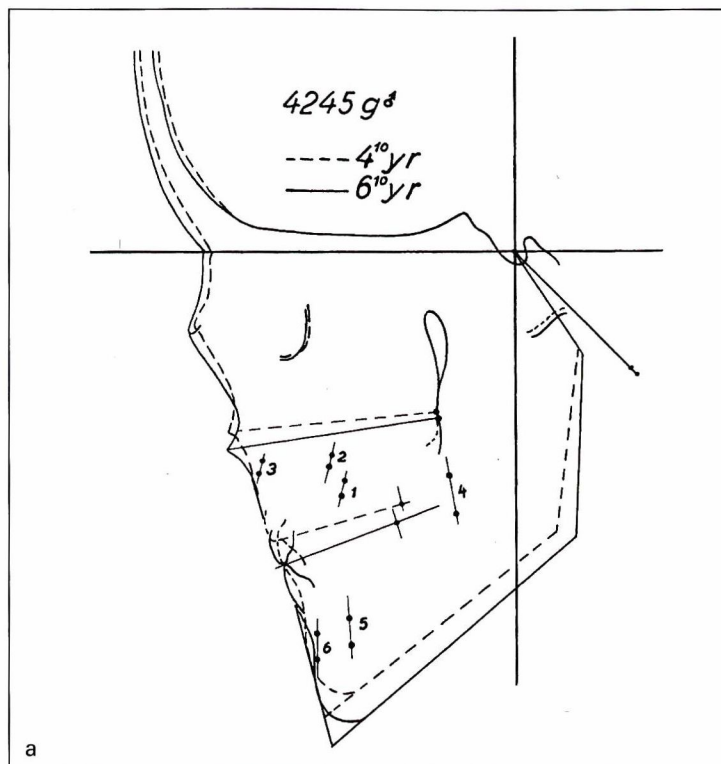


Fig 1-39a General superimposition of the first case published by Björk²⁶ in 1955—boy 4245 g—reprinted in its original form. Superimposition is on the anterior cranial base. The lines connecting the implants demonstrate, in lateral projection, the shift in space of the six implants in the 2-year period between the ages of 4 years 10 months and 6 years 10 months. Note the difference in the direction of shifting between maxillary implants (1, 2, 3) and mandibular implants (4, 5, 6). Björk used the initial sella-nasion (S-Na) line as a horizontal reference (instead of Frankfort horizontal) and S-Na perpendicular line as a sagittal reference. (Reprinted from Björk²⁶ with permission.)

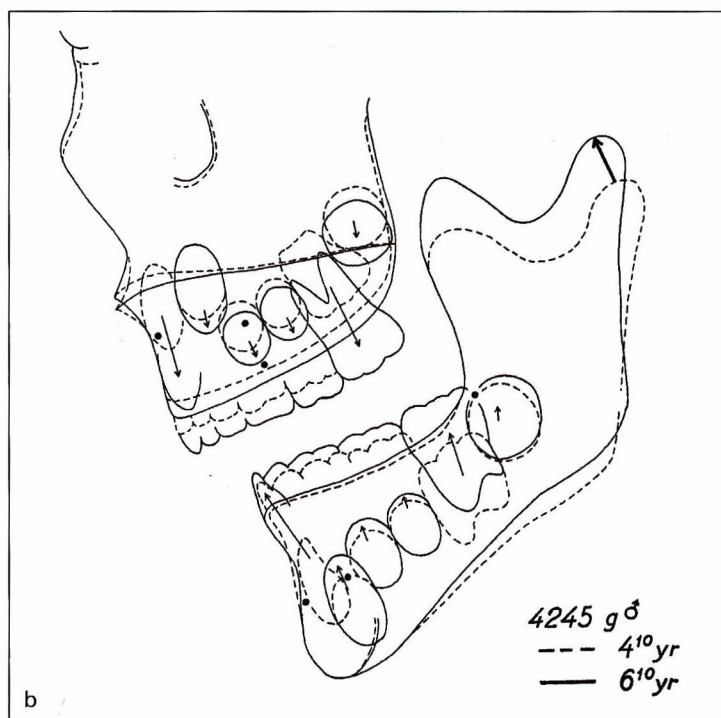


Fig 1-39b Very first local superimpositions of the maxillary and mandibular tracings on metallic implants placed in a human child (boy 4245 g). Bone deposition is visible in the vertical and posterior directions in the maxilla at the alveolar ridge and the tuberosity region. In the anterior region, no sagittal deposition can be seen. The nasal floor demonstrates resorption, with downward and slightly forward remodeling of the anterior nasal spine. The lowering of the maxilla is accompanied by deposition at the floor of the orbit. The vertical sutural additions to the height of the maxillary frontal process can be estimated by the increase observed at the nasofrontal suture. The lowering of the maxilla due to sutural growth can be estimated by the shift of the implants 1, 2, and 3 (see Fig 1-39a). The direction of growth of the condyle is upward and forward. Deposition of bone can be seen at the mandibular alveolar ridge, and there is a frontal area of periosteal resorption above the chin region, where there is no deposition of bone. Resorption can be seen at the gonial region and the upper part of the posterior surface of the ramus. This first superimposition with implants in essence demonstrated the differences between Björk's implant studies and the procedures used by Broadbent^{39,68} and Brodie.⁷³ (Reprinted from Björk²⁶ with permission.)

facial form develop and clarified their impact on the development of malocclusions. The need to understand the influence of the individual growth pattern on treatment outcome became evident. Facial form and its changes are compared with the patient and are largely independent from population-derived standards.

Identification of natural reference markers

Björk's investigations identified the location of natural reference markers in the anterior cranial base, the mandible, and the maxilla. Natural reference markers can be used for the superimposition of the anterior cranial base, the maxilla, and the mandible of patients in whom no implants have been placed. This made the method accessible for clinicians and researchers to investigate treatment outcomes in patients.

Again, it should be stressed that the structural method is fundamentally different from all other methods of superimposition because it is evidence-based. The method uses natural internal structures present in the bones of the individual and visible on serial films. It is independent of the use of landmarks or planes and of comparisons with population-derived standards. Chapter 2 deals with the natural reference markers in great detail.

Prediction of facial growth

There was great hope for facial growth prediction between 1970 and 1985. A possible impetus for that optimism came from the clinically successful prediction of total body height.¹¹³ The hypothesis was that the initial cephalogram of a patient contained hidden, detailed information on how the face would grow. That hypothesis was also more or less derived from Brodie's opinion^{73,114} that the growth pattern of the human head, once established in early childhood, does not change and that orthodontic treatment would be limited to changes in the alveolar processes. If that hidden information could be retrieved and compared with an appropriate database, prediction would be so precise that it could determine the plan and outcome of treatment. Prediction methods were designed in several ways, mostly based on population averages,¹¹⁵ and the design of a visual treatment objective (VTO)—the superimposition of the pretreatment tracing and the designed prognostic tracing—became part of treatment-planning procedures.⁴¹

The prediction method developed by the Ricketts group⁴¹ was based on averages of change per year (and their standard deviations) over a 5-year period in a number of well-known cephalometric variables resulting from the analysis of the group's record collection. It was assumed that in the individual patients for whom prediction would have to be done, change would be within 1 standard deviation. The VTO was superimposed on the nasion-basion line.

Both of those reference points are unstable and change with growth (see Figs 1-28 and 1-29). Greenberg and Johnston¹¹⁶ questioned the utility of these procedures in patients in whom growth was a significant factor during treatment. They concluded that the method showed serious flaws, and prediction proved unreliable.

Even in the early 1960s, with the insights gained from the implant studies, the Copenhagen researchers expected that prediction could be so precise that the initial cephalo-

gram could be used in that way.⁵⁸ Björk⁹⁶ elaborated on the idea further in 1969, when he suggested that certain internal bony structures could be used for the prediction of the growth pattern and that these were more useful than angular measurements. He presented seven structural signs of extreme growth rotation. These structural signs were supposed to correlate with the direction of the condylar growth.

Ari-Viro and Wisth¹⁰² evaluated the method of structural growth prediction proposed by Björk. A team of 11 observers evaluated the initial cephalogram of 42 children using the anatomical characteristics indicated by Björk. The interobserver and intraobserver reliability was acceptable. Mandibular rotation was determined on cephalograms of the same children at 4-year intervals. There was no absolute correlation between the scores of different criteria and mandibular rotation. Ari-Viro and Wisth¹⁰² concluded that the method did not work well in patients with relatively small rotational changes and suggested further study using extreme cases.

Skieller and co-workers¹¹⁷ explored the prediction of mandibular growth rotation in a retrospective study of implant cases. They selected 21 individuals with extreme growth patterns from a group of 100 children. A growth prediction procedure was designed based on 10 morphologic characteristics. However, the results were discouraging: Only for extreme cases was prediction of clinical significance.¹¹⁸

Baumrind et al¹¹⁹ reported the results of an experimental study in which a team of experts tried to predict mandibular growth rotation in selected patients with moderate growth patterns. The experts failed to do better than chance. An evaluation of the Skieller prediction method by the Baumrind team¹²⁰ on a different sample of patients with implants showed the method to be less successful. The team nevertheless concluded that clinicians were made aware of the complexities of predicting growth patterns in individual cases.

In a further study,¹¹⁹ the prediction of mandibular rotation using 4 of the 10 morphologic characteristics of the Skieller method¹¹⁷ was assessed in a sample of 40 randomly selected, untreated adolescents. Statistical analysis showed that clinically useful prediction of future mandibular growth rotation in a general population was not possible.

Chvatal et al¹²¹ designed a new prediction procedure and concluded that longitudinal growth curves based on multilevel procedures can accurately describe population and individual growth curves in persons for whom longitudinal data are available. The longitudinal growth curves they developed are based on a longitudinal cephalogram series of 159 girls and 128 boys. The authors claim that 5-year predictions with this method are highly accurate. The procedure appears promising for extreme growth patterns.

Von Bremen and Pancherz¹²² tested the structural signs of mandibular growth rotation in a single pretreatment cephalogram, as indicated by Björk, to see how well their presence could be used for diagnostic purposes. The questions asked were: (1) Is specific mandibular morphology related to hyperdivergent or hypodivergent forms? (2) Are severely deviant forms more easily detected than mild ones? (3) Is that age related? The subject group consisted of 135 Class I or Class II individuals; of these, 95 individuals exhibited a large (> 38 degrees) and 40 individuals had a small (< 26 degrees) mandibular plane angle (intersection of the mandibular plane and the sella-nasion line).

On two occasions, nine observers judged mandibular cuttings from the lateral cephalograms. The observers, who

were unaware of the actual skeletofacial morphology, had to categorize the mandibular cuttings as belonging to either hypodivergent or hyperdivergent faces. The results showed that it was difficult to categorize subjects as either hypodivergent or hyperdivergent on the basis of mandibular morphology. Age was not a factor. Hypodivergency was easier to identify than hyperdivergency.

In summary, it must be stated that facial growth prediction using the initial lateral cephalogram—with the exception of extreme cases—seems to have limited potential. It appears that the cephalogram of the average patient does not contain the data necessary for clinically useful prediction. The reasons for this are not easily explained. The multitude of genetic, epigenetic, and environmental factors controlling skeletofacial morphology in future space and time might not express themselves sufficiently to be detectable in the abstraction of a child's lateral cephalogram. The process of growth rotation as described by Björk seems to be a process that occurs to an appreciable amount only in extreme cases. It may be that morphologic deviants participate in that process variably in time, location, direction, and amount. A somewhat similar phenomenon has been observed in facial asymmetry where patients showed progressive, decreasing, or stable asymmetry.¹²³ The final conclusion by Von Bremen and Pancherz¹²² that morphologic growth prediction using mandibular structural signs has to be regarded with skepticism is justified. When longitudinal records of a patient are available, prediction might be more accurate, as the findings by Chvatal et al¹²¹ show.

Again, it must be realized that the head is the most complicated structure of the human body, and many factors determining details of its morphology are not yet understood. This does not mean that information from the initial cephalogram is useless. Careful and thoughtful consideration of a patient's facial form characteristics alerts and sensitizes the clinician to be cautious when considering treatment solutions and results. The cogent comment by Baumrind et al¹¹⁹ also reminds us of a different reality: Orthodontists seem to rely more on continual observation of treatment progress to monitor prediction than on the use of pretreatment records.

Recent commercial developments

Several different superimposition methods have been used in commercially available software programs. Not all of these methods have identical merits. With the scientific basis available, improved radiographic techniques, and advanced computer applications, an evidence-based choice should be made; the obvious choice is the structural method. All other superimpositions may be useful as illustrations to highlight a pretreatment or posttreatment difference, but they are unsuitable for interpreting what occurred during growth and/or treatment in a single patient.

Conclusion

As is the case with every scientific method in biology, the structural method of superimposition is accompanied by uncertainties and limitations. However, the structural method is the best approach available because it is evidence-based; all other methods lack any foundation of evidence.

There is no legitimate reason for orthodontic professionals to continue on the basis of tradition or convention with the clinical use, teaching, or acceptance of published methods that have been shown to be invalid.

The intricacies of the structural method, its evidence base, and details related to its background are extensively reviewed in chapter 2. Execution of the structural method of superimposition requires specific knowledge and training, a topic reviewed in chapters 3 through 6. Application of the method is demonstrated in chapters 7 and 8.

References

1. Gijssels C. La Naissance de la Morphologie Dento-Faciale. Paris: Société Française d'Orthopédie Dento-Faciale, 1980.
2. Hunter J. The Natural History of the Human Teeth: Explaining Their Structure, Use, Formation, Growth and Diseases. London: J. Johnson, St Paul's Churchyard, 1771.
3. Belchier J, Goodsir J. The classic: An account of the bones of animals being changed to a red colour by aliment only. 1966. Clin Orthod Relat Res 2006;443:11–13.
4. Duhamel du Monceau HL. Sur une racine qui a la faculté de teindre en rouge les os des animaux vivants. Mémoires de l'Académie Royale des Sciences de Paris 1739:1–13.
5. Von Kolliker RA. Die Normale Resorption des Knochengewebes und ihre Bedeutung für die Entstehung des Typischen Knochenformen. Leipzig: FCW Vogel, 1873.
6. Humphry GM. On the growth of the jaws. Trans Cambridge Philos Soc 1866;11:1–5.
7. Enlow DH. Principles of Bone Remodeling. Springfield, IL: Charles C. Thomas, 1963.
8. Baer MJ, Bosma JF, Ackerman JL. The Postnatal Development of the Rat Skull. Ann Arbor, MI: University of Michigan Press, 1983.
9. Brash JC. The Growth of the Jaws and Palate. London: Dental Board of the United Kingdom, 1924.
10. Brash JC. Some problems in the growth and developmental mechanics of bone. Edinb Med J 1934;41:305,363–387.
11. Moore AW. Head growth of the macaque monkey as revealed by vital staining, embedding and undecalcified sectioning. Am J Orthod 1949;35:654–671.
12. Hoyte DAN. Experimental investigations of skull morphology and growth. In: Felts WJL, Harrison RJ (eds). International Review of General and Experimental Zoology, vol 2. New York: Academic Press, 1966:345–407.
13. Hoyte DAN. The modes of growth of the neurocranium: The growth of the sphenoid bone in animals. In: Moyers RE, Krogman WM (eds). Cranio-Facial Growth in Man. New York: Pergamon Oxford, 1971:77–105.
14. Duterloo HS, Vilmann H. Translative and transformative growth of the rat mandible. Acta Odontol Scand 1978;36:25–32.
15. Massler M. The Growth Pattern of the Cranial Vault in the Albino Rat As Measured by Vital Injections of Alizarin Red "S" [thesis]. Chicago: University of Illinois, 1941.
16. Massler M. The postnatal growth pattern of the cranium as measured by vital injections of alizarin red S. J Dent Res 1944;23:193–194.
17. Vilmann H. The growth of the cranial base in the albino rat studied by vital staining with alizarin red S. Acta Odontol Scand Suppl 1971;29(59):1–44.
18. Vilmann H. Neurokraniets vækst på Wistar Albinorotten undersøgt med Røntcefalometri og Vitalfarvning med Alizarin Red S: An Undersøgelse af Knoglevækstprincipper [thesis]. Copenhagen: University of Copenhagen, 1973.

1 History and Origin of the Structural Method

19. Henry HL. An experimental study of external force application to the maxillary complex. In: McNamara JA Jr (ed). *Factors Affecting the Growth of the Midface*, monograph 6, Craniofacial Growth Series. Ann Arbor, MI: University of Michigan, 1976:301–326.
20. McNamara JA Jr. Neuromuscular and skeletal adaptations to altered function in the orofacial region. *Am J Orthod* 1973;64:578–606.
21. Moffett B. Remodelling of the craniofacial articulations by various orthodontic appliances in rhesus monkeys. *Eur Orthod Soc* 1971;207–216.
22. Moffett BC. Remodeling changes of the facial sutures, periodontal and temporomandibular joints produced by orthodontic forces in rhesus monkeys. *Bull Pac Coast Soc Orthod* 1969;44:46–49.
23. Duterloo HS. *Extra Orale Tractie*. Alphen aan den Rijn, The Netherlands: Stafleu & Tholen, 1981.
24. Meikle MC. *Craniofacial Development, Growth and Evolution*. Norfolk, UK: Bateson, 2002.
25. Herring S. How can animal models answer clinical questions? In: Carels C, Willems G (eds). *The Future of Orthodontics*. Leuven, Belgium: Leuven University Press, 1998:89–97.
26. Björk A. Facial growth in man, studied with the aid of metallic implants. *Acta Odontol Scand* 1955;13:9–34.
27. Björk A. The face in profile. *Sven Tandläk Tidskr* 1947;40(suppl 5B).
28. Camper P. *Dissertation physique sur les différences réelles qui présentent les traits du visage chez les hommes de différents pays et de différents âges. Sur le beau qui caractérise les statues antiques et les pierres gravées. Suivie de la proposition d'une Nouvelle Méthode pour dessiner toutes sortes de têtes humaines avec la plus grande sûreté*. Utrecht: B Wild & J Altheer, 1791.
29. Gijssels C. *Histoire de l'Orthodontie: Ses Origines, son Archéologie et ses Précurseurs*. Brussels: Société Belge d'Orthodontie, 1997.
30. Meijer MC. *Race and Aesthetics in the Anthropology of Petrus Camper (1722–1789)*. Amsterdam: Rodopi, 1999.
31. Dürer A. *Hierin sind begriffen vier Bücher von menschlicher Proportion*. Nuremberg, Hieronymus Andreae 1528.
32. Van Loon JAW. A new method for indicating normal and abnormal relations of teeth to the facial lines. *Dent Cosmos* 1915;57:973, 1093, 1229.
33. Moorrees CFA. Cephalometry and orthodontics after the introduction of Van Loon's "cubus cranioforus" [in Dutch]. *Ned Tijdschr Tandheelkd* 1988;95:461–467.
34. Gijssels C. *Conférence autour de Camper (1722-1789) et de son angle facial*. *L'Orthodontie Française* 1980;51:59–97.
35. Gould SJ. *The Mismeasure of Man*. London: WW Norton, 1996.
36. Gould SJ. Petrus Camper's angle: The grandfather of scientific racism has gotten a bum rap. *Nat Hist* 1987;96:12–16.
37. Leroy AM. *Mutants: On the Form, Varieties and Errors of the Human Body*. London: Harper Collins, 2003.
38. Welcker H. *Untersuchungen über Bau und Wachstum des menschlichen Schädels*. Leipzig: Erster Teil, 1862.
39. Broadbent BH. The face of the normal child. *Angle Orthod* 1937;7:183–208.
40. Ricketts RM. A four-step method to distinguish orthodontic changes from natural growth. *J Clin Orthod* 1975;9:208–215, 218–228.
41. Ricketts RM, Bench RW, Gugino CF, Hilgers JJ, Schulhof RJ. *Bioprogessive Therapy*. Denver: Rocky Mountain Orthodontics, 1979.
42. Keith A, Campion G. A contribution to the mechanism of growth of the human face. *Int J Orthod* 1922;8:607–633.
43. Hellman M. The face in its developmental career. *Dent Cosmos* 1935;77:685–787.
44. Moyers RE. *Handbook of Orthodontics: For the Student and General Practitioner*. Chicago: Year Book, 1958.
45. Moyers RE. *Handbook of Orthodontics*, ed 4. Chicago: Year Book, 1988.
46. Hunter WS, Carlson DS (eds). *Essays in Honor of Robert E. Moyers*. Ann Arbor, MI: University of Michigan, 1991:24.
47. Keith A. *An Autobiography*. London: Watts, 1950.
48. Enlow DH. *The Human Face: An Account of the Postnatal Growth and Development of the Craniofacial Skeleton*. New York: Hoeber Medical Division, 1968.
49. Enlow DH. *Handbook of Facial Growth*. Philadelphia: Saunders, 1975.
50. Moss ML. The functional matrix. In: Kraus BS, Riedel RA (eds). *Visitas in Orthodontics*. Philadelphia: Lea & Febiger, 1962:85–98.
51. Scott JH. *Dento-Facial Development and Growth*. Oxford: Pergamon Press, 1967.
52. van Limborgh J. A new view on the control of the morphogenesis of the skull. *Acta Morphol Neerl Scand* 1970;8:143–160.
53. Weinmann JP, Sicher H. *Bone and Bones*. St Louis: Mosby, 1947.
54. Enlow DH, Bang S. Growth and remodeling of the human maxilla. *Am J Orthod* 1965;51:446–464.
55. Björk A. Sutural growth of the upper face studied by the implant method. *Acta Odontol Scand* 1966;24:109–127.
56. Björk A, Skieller V. Postnatal growth of and development of the maxillary complex. In: McNamara JR JA (ed). *Factors Affecting the Growth of the Midface*, monograph 6, Craniofacial Growth Series. Ann Arbor, MI: University of Michigan, 1976:61–99.
57. Melsen B. Histological analysis of the postnatal development of the nasal septum. *Angle Orthod* 1977;47:83–97.
58. Björk A. Variations in the growth pattern of the human mandible: Longitudinal radiographic study by the implant method. *J Dent Res* 1963;42(1 pt 2):400–411.
59. Trinkaus E, Shipman P. *The Neanderthals: Changing the Image of Mankind*. London: Jonathan Cape, 1993.
60. Scharf JH. Die erste röntgenaufnahme eines menschlichen Schädels. *Biol Rundsch* 1972;10:202–205.
61. Welcker H. Das Profil des menschlichen Schädels mit Röntgenstrahlen am Lebenden dargestellt. *Deutsche Gesellschaft für Anthropologie Ethnologie Urgeschichte* 1896;27:38–39.
62. Todd TW. *Atlas of Skeletal Maturation of the Hand*. St Louis: Mosby, 1937.
63. Hofrath H. Die Bedeutung der Röntgenfern- und Abstandsaufnahme für die Diagnostik der Kieferanomalien. *Fortschr Kieferorthop* 1931;1:232–258.
64. Broadbent BH. A new X-ray technique and its application to orthodontia. *Angle Orthod* 1931;1:45–66.
65. Krogman WM, Sassouni V. *A Syllabus in Roentgenographic Cephalometry*. Philadelphia: Wiley, 1957.
66. Bruhn C, Hofrath H, Korkaus G (eds). *Handbuch der Zahnheilkunde*, vol 4. *Gebiss-, Kiefer- und Gesichtorthopädie*. Munich: JF Bergmann, 1939.
67. Hofrath H. Die Röntgenographie im Dienste der Gebiß- und Kieferorthopädie. In: Bruhn C, Hofrath H, Korkhaus G (eds). *Handbuch der Zahnheilkunde*, vol 4. *Gebiss-, Kiefer- und Gesichtorthopädie*. Munich: JF Bergmann, 1939:1064–1143.
68. Broadbent BH Sr, Broadbent BH Jr, Golden WH. *Bolton Standards of Dentofacial Developmental Growth*. St Louis: Mosby, 1975.
69. Pacini AJ. Roentgen ray anthropometry of the skull. *J Radiol* 1922;230–238, 322–331, 418–426.
70. Allen WI. Historical aspects of roentgenographic cephalometry. *Am J Orthod* 1963;49:451–459.
71. Krogman WM. The problem of growth changes in the face and skull of anthropoids and man. *Dent Cosmos* 1930;72:624–630.
72. Behrens RG. A Treatise on the Continuum of Growth in the Aging Craniofacial Skeleton [thesis]. Ann Arbor, MI: University of Michigan, 1984.
73. Brodie AG. On the growth pattern of the human head from the third month to eight years of life. *Am J Anat* 1941;68:209–262.
74. Greulich WW, Pyle SI. *Radiographic Atlas of Skeletal Development of the Hand and Wrist*. Stanford: Stanford University Press, 1950.
75. Pyle SI, Hoerr N.L. *Radiographic Atlas of Skeletal Development of the Knee: A Standard of Reference*. Springfield, IL: Charles C. Thomas, 1955.
76. Riolo ML, Moyers RE, McNamara JA Jr, Hunter WS. *An Atlas of Craniofacial Growth*, monograph 2, Craniofacial Growth Series. Ann Arbor, MI: University of Michigan, 1974.

77. Kamoen A, Dermaut L, Verbeeck R. The clinical significance of error measurement in the interpretation of treatment results. *Eur J Orthod* 2001;23:569–578.
78. Baumrind S, Ben-Bassat Y, Bravo LA, Curry S, Korn EL. Partitioning the components of maxillary tooth displacement by the comparison of data from three cephalometric superimpositions. *Angle Orthod* 1996;66:111–124.
79. Björk A, Skieller V. Facial development and tooth eruption: An implant study at the age of puberty. *Am J Orthod* 1972;62:339–383.
80. Pancherz H, Fischer S. Amount and direction of temporomandibular joint growth changes in Herbst treatment: A cephalometric long-term investigation. *Angle Orthod* 2003;73:493–501.
81. Moorrees FA, Kent RL, Efstratiadis SS, Reed RB. Components of landmark movement during facial growth. In: *Study Week. Nederlandse Vereniging Orthodontische Studie*, 1985:55–70.
82. Moorrees CFA. Twenty centuries of cephalometry. In: Jacobson A, Jacobson RL (eds). *Radiographic Cephalometry: From Basics to 3-D Imaging*. Chicago: Quintessence, 2006:13–32.
83. Thompson DW. *On Growth and Form*. Dover reprint of 1942, ed 2. Cambridge: Cambridge University Press, 1992.
84. Bastir M, Rosas A, O'Higgins P. Craniofacial levels and the morphological maturation of the human skull. *J Anat* 2006;209:637–654.
85. Weber GW, Bookstein FL. *Virtual Anthropology: A Guide to a New Interdisciplinary Field*. Vienna: Springer, 2011.
86. Lieberman DE. Sphenoid shortening and the evolution of modern human cranial shape. *Nature* 1998;393:158–162.
87. Lieberman DE, Pearson OM, Mowbray KM. Basicranial influence on overall cranial shape. *J Hum Evol* 2000;38:291–315.
88. Spoor F, O'Higgins P, Dean C, Lieberman DE. Anterior sphenoid in modern humans. *Nature* 1999;397:572.
89. Duterloo HS, Planché P-G. *An Illustrated Guide to Prepare for the Examination of the European Board of Orthodontists*, Edition 2005. European Orthodontic Society. <http://www.eoseurope.org/documents/instructions/EBO05.pdf>. Accessed 9 July 2009.
90. Steiner C. Cephalometrics in clinical practice. *Angle Orthod* 1959;29:8–29.
91. Downs WB. The role of cephalometrics in orthodontic case analysis and diagnosis. *Am J Orthod* 1952;38:162–182.
92. Tweed CH. Evolutionary trends in orthodontics: Past, present, and future. *Am J Orthod* 1953;39:81.
93. Tweed CH. The Frankfort-mandibular incisor angle (FMIA) in orthodontic diagnosis, treatment planning and prognosis. *Angle Orthod* 1954;24:121–169.
94. McNamara Jr JA, Brudon WL. *Orthodontic and Orthopedic Treatment in the Mixed Dentition*. Ann Arbor, MI: Needham Press, 1993.
95. De Coster L. The familial line, studied by a new line of reference. *Trans Eur Orthod Soc* 1952;28:50–55.
96. Björk A. Prediction of mandibular growth rotation. *Am J Orthod* 1969;55:585–599.
97. Björk A, Skieller V. Normal and abnormal growth of the mandible: A synthesis of longitudinal cephalometric implant studies over a period of 25 years. *Eur J Orthod* 1983;5:1–46.
98. Ricketts RM. Divine proportion in facial esthetics. *Clin Plast Surg* 1982;9:401–422.
99. Ricketts RM. *Provocations and Perceptions in Craniofacial Orthopedics*, vol 1. San Diego: Jostens USA, 1989:817–818.
100. Melsen B. The cranial base: The postnatal development of the cranial base studied histologically on human autopsy material. *Acta Odontol Scand Suppl* 1974;32(62):1–126.
101. Björk A. Kæbernes relation til det øvrige kranium. In: Lundström A (ed). *Nordisk Lärobok i Ortodonti*. Stockholm: Sveriges Tandläkarförbunds Förlagsforening, 1975:70–75.
102. Ari-Viro A, Wisth PJ. An evaluation of the method of structural growth prediction. *Eur J Orthod* 1983;5:199–207.
103. Buschang PH, LaPalme L, Tanguay R, Demirjian A. The technical reliability of superimposition on cranial base and mandibular structures. *Eur J Orthod* 1986;8:152–156.
104. Cook AH, Sellke TA, Begole EA. The variability and reliability of two maxillary and mandibular superimposition techniques. 2. *Am J Orthod Dentofacial Orthop* 1994;106:463–471.
105. Cook PA, Gravely JF. Tracing error with Björk's mandibular structures. *Angle Orthod* 1988;58:169–178.
106. Dibbets JM. A method for structural mandibular superimpositioning. *Am J Orthod Dentofacial Orthop* 1990;97:66–73.
107. Dibbets JMH. Comment on superimposition technique. *Am J Orthod Dentofacial Orthop* 1994;107:18A–19A.
108. Swarz ML. Comment on superimposition techniques. *Am J Orthod Dentofacial Orthop* 1995;107:6,17A.
109. Arat ZM, Rübendüz M, Akgül AA. The displacement of craniofacial reference landmarks during puberty: A comparison of three superimposition methods. *Angle Orthod* 2003;73:374–380.
110. Springate SD, Jones AG. The validity of two methods of mandibular superimposition: A comparison with tantalum implants. *Am J Orthod Dentofacial Orthop* 1998;113:263–270.
111. Lacroix P. *The Organization of Bones*. London: Churchill, 1951.
112. Theunissen JJW. *Het Fibreuze Periosteum* [thesis]. Nijmegen, The Netherlands: University of Nijmegen, 1973.
113. Tanner JM. *Growth at Adolescence*, ed 2. Oxford: Blackwell, 1962.
114. Brodie AG. Late growth changes in the human face. *Angle Orthod* 1953;23:146–157.
115. Schulhof RJ, Bagha L. A statistical evaluation of the Ricketts and Johnston growth-forecasting methods. *Am J Orthod* 1975;67:258–276.
116. Greenberg LZ, Johnston LE. Computerized prediction: The accuracy of a long-range forecast. *Am J Orthod* 1975;67:243–252.
117. Skieller V, Björk A, Linde-Hansen T. Prediction of mandibular growth rotation evaluated from a longitudinal implant sample. *Am J Orthod* 1984;86:359–370.
118. Ekström C. Facial growth rate and its relation to somatic maturation in healthy children. *Swed Dent J Suppl* 1982;11:1–99.
119. Baumrind S, Korn EL, West EE. Prediction of mandibular rotation: An empirical test of clinician performance. *Am J Orthod* 1984;86:371–385.
120. Lee RS, Daniel FJ, Swartz M, Baumrind S, Korn EL. Assessment of a method for the prediction of mandibular rotation. *Am J Orthod Dentofacial Orthop* 1987;91:395–402.
121. Chvatal BA, Behrents RG, Ceen RF, Buschang PH. Development and testing of multilevel models for longitudinal craniofacial growth prediction. *Am J Orthod Dentofacial Orthop* 2005;128:45–56.
122. von Bremen J, Pancherz H. Association between Björk's structural signs of mandibular growth rotation and skeletofacial morphology. *Angle Orthod* 2005;75:506–509.
123. Pirttiniemi P, Miettinen J, Kantomaa T. Combined errors in frontal-view asymmetry diagnosis. *Eur J Orthod* 1996;18:629–636.

Validity and Reliability: Method Error

The structural method usually incorporates three different superimpositions: (1) general superimposition on the anterior cranial base, (2) local superimposition of the mandible, and (3) local superimposition of the maxilla. Each of these superimpositions has specific limitations related to method error. Insight into method error becomes particularly relevant if the time interval between the cephalograms is relatively short and the changes brought about by growth and treatment are relatively small. Such is often the case in the evaluation of orthodontic patients. The following sections discuss the method error of each of the three superimpositions with regard to their *validity* (ie, biologic significance) and *reliability* (ie, precision and accuracy). In addition to local superimpositions of the mandible and maxilla, regional superimpositions¹⁻⁴ are also used to investigate changes in the position of the mandible relative to the maxilla and vice versa. The validity and reliability of that procedure depends on (1) the validity and reliability of local superimposition of either the mandible or the maxilla and (2) the accuracy of registration of the occlusion. This chapter does not address the topic of regional superimposition.

Most studies on reliability predate the era when advanced computerized manipulation of radiographs became possible. Nevertheless, they provide the logical basis for work with newer digital methods. Chapters 7 and 8 address the practical aspects of structural superimposition.

Method Error in Structural Superimposition on the Cranial Base

Validity of structural superimposition on the cranial base

The validity of general superimposition using the structural method with natural reference markers is largely based on the histologic investigations of Melsen.⁵ The principal findings of that study are summarized in Fig 2-1.

The application of structural anterior cranial base superimposition requires thorough knowledge of the anatomy of the region and how it is imaged in the cephalogram (Figs 2-2 to 2-7). The clinical significance of the results by Melsen⁵ is the finding that two relatively distant structures are stable after the age of 6 years. The anterior part of the sella turcica (see Fig 2-1, surface 5) can be used to register the superimposed tracing in a horizontal direction, while the cribriform plate of ethmoid bone and the squamous part of the frontal bone (see Fig 2-1, surfaces 1 and 2) can be used to orient the superimposed tracing in a vertical direction. This can eliminate rotational errors to a large extent.

In many publications, only surfaces 3, 4, and 5 in Fig 2-1 are used for a best-fit superimposition, but the use of only these contours is not recommended for two reasons. First, the endocranial (meningeal) periosteal surface of the jugum

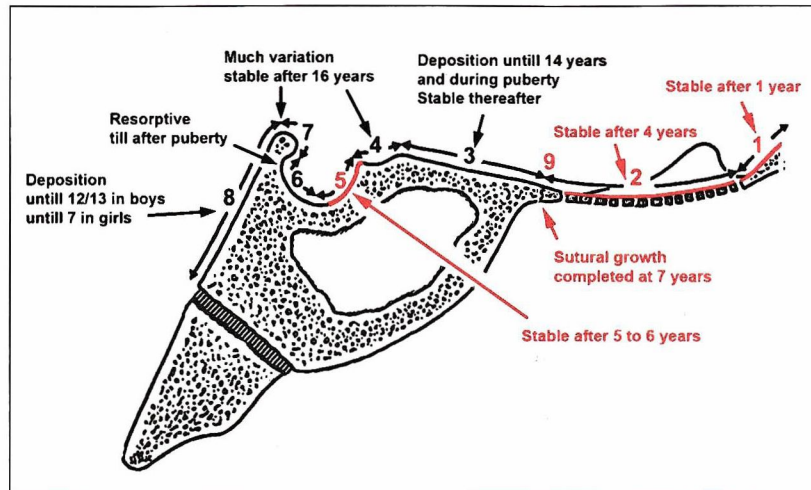


Fig 2-1 Stable surfaces useful for structural superimposition on the anterior cranial base are indicated in red. 1. Cerebral surface of the squamous part of the frontal bone; 2. lamina cribrosa of the ethmoid bone; 3. jugum of the sphenoid bone; 4. sulcus chiasmatis and tuberculum sellae; 5. anterior part of sella turcica; 6. posterior part of sella turcica; 7. anterior part of the dorsum sellae; 8. anterior part of clivus; 9. sphenoethmoidal suture. Data based on a carefully documented autopsy study of the histology of the midline structures of the cranial base from 76 males and 50 females aged between 0 and 20 years. (Adapted from Melsen⁵ with permission.)

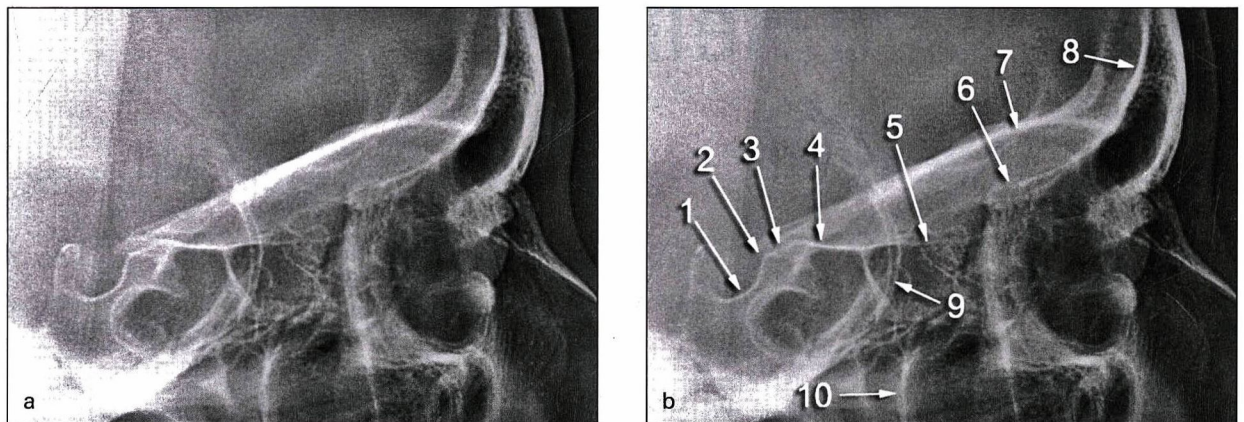


Fig 2-2 (a and b) Details of the anterior cranial base in a cephalogram. 1. Anterior wall of the pituitary fossa (sella turcica); 2. point where the anterior wall of the pituitary fossa crosses the inferior surface of the anterior clinoid process (Walker point⁶); 3. sulcus chiasmatis, tuberculum sellae, and the jugum of the corpus of sphenoid bone; 4. jugum of sphenoid bone, crossed by the greater wings; 5. lamina cribrosa of ethmoid bone; 6. cerebral surface of the roof of ethmoidal air cells (ethmoidal crest); 7. orbital surface of the orbital part of the frontal bone (roof of orbita); 8. cerebral surface of the squamous part of the frontal bone; 9. greater wings of the sphenoid; 10. anterior wall of the pterygoid fossa (formed by the maxillary tuberosity). The anterior wall of the pituitary fossa (1) and Walker point (2) are very visible and used for orientation superimposition because they are reported to be stable very early in life. The cribriform plate (5) is the most inferior of three contours: the orbital roof (7), the ethmoidal crest (6), and the cribriform plate (5). It is often rather indistinct but can be found by starting at the jugum (4), where the greater wings (9) cross, and following slightly downward, not upward, because the cribriform plate lies in a recess between the uppermost ethmoidal air cells and the ethmoidal crests. Double images are normally seen in the anterior cranial base region; the most common are (9) and (7) (see chapter 4). The orbital surface of the roof of the orbita (7) is clearly visible in cephalograms. It is often erroneously included in tracings as if continuous from the sulcus chiasmatis (3) and then used for superimposition. However, it is not a midline cranial base structure. The cerebral surface of the roof of the orbita is often indistinct due to the projection of impressiones gyrorum and juga cerebraalia. The cerebral orbital surface is resorptive and the orbital surface is depository during anterior-directed displacement growth of the orbits.⁷ The age at which growth changes of these surfaces cease is not entirely clear. These structures cannot be recommended for anterior cranial base superimposition.

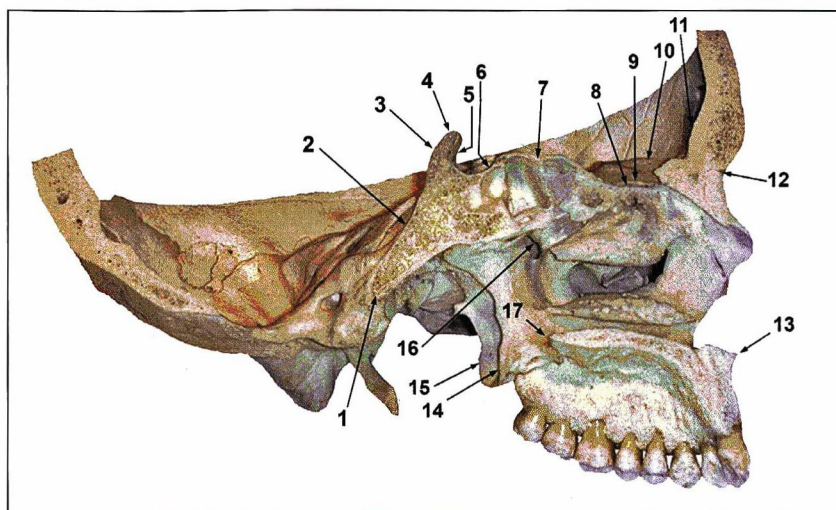


Fig 2-3 Median sagittal section of the adult skull (left half, with the nasal septum and the vomer removed) showing the cranial base and facial midline structures as observed in lateral cephalograms. The labeled structures are selected on the basis of their visibility in cephalograms and their significance in relation to the cephalometric tracing technique and structural superimposition. 1. Anterior rim of the foramen magnum of the basilar part of the occipital bone; 2. clivus; 3. dorsum sellae; 4. posterior clinoid process; 5. posterior wall of the pituitary fossa (sella turcica); 6. anterior wall of the pituitary fossa and tuberculum sellae; 7. jugum of the sphenoid bone; 8. lamina cribrosa of ethmoid bone; 9. cerebral surface of the roof of the ethmoidal air cells; 10. cerebral surface of the orbital part of the frontal bone; 11. frontal crest of the frontal bone; 12. frontonasal suture; 13. anterior nasal spine; 14. posterior rim of the medial pterygoid plate; 15. posterior rim of the lateral pterygoid plate; 16. sphenopalatine foramen; 17. posterior nasal spine. The sphenopalatine foramen (16) is formed by the sphenopalatine notch at the upper end of the perpendicular plate of the palatine bone and the body of the sphenoid. The foramen is often visible in cephalograms at the upper limit of the pterygopalatine fossa (pterygomaxillary fissure). Posterior nasal spine (17) is formed where the posterior limits of the horizontal parts of the right and left palatine bones meet at the median palatine suture.

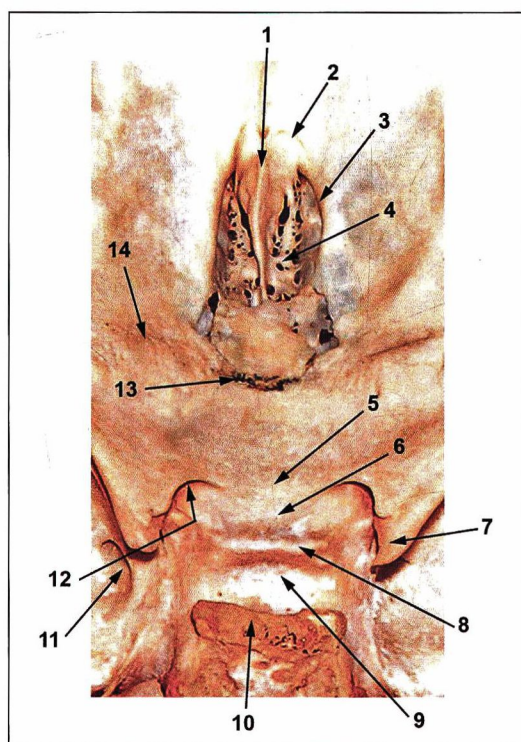


Fig 2-4 Internal surface (viewed from above) of the anterior cranial base in the skull of a child aged about 8 years. 1. Crista galli; 2. frontoethmoidal suture; 3. roof of the ethmoidal air cells; 4. cribriform plate of ethmoid bone; 5. jugum of the sphenoid bone; 6. sulcus chiasmatis (prechiasmatic groove); 7. anterior clinoid process; 8. tuberculum sellae; 9. pituitary fossa; 10. posterior clinoid process; 11. foramen rotundum; 12. optic canal; 13. sphenothmoidal suture; 14. sphenofrontal suture. The crista galli (1) of the ethmoid bone is a small, thin, vertical midline plate projecting upward between the cribriform plates. In life, it is connected to the falx cerebri. The crista galli is only occasionally visible in cephalograms. The jugum of the sphenoid bone (5) is the flat cerebral surface of the body of the sphenoid. It is usually easily visible in cephalograms and often used for superimposition. Melsen,⁵ however, noted continuous bone deposition during puberty until 14 years of age (see Fig 2-1). Systematic incorporation of the jugum in structural superimposition of the anterior cranial base procedure is not recommended. The sphenothmoidal suture (13) is the articulation between the body of the sphenoid and the ethmoid bone. The sphenofrontal suture (14) is the articulation between the lesser wing of the sphenoid and the orbital part (roof) of the frontal bone. Both sutures appear to be still open, indicating possible growth activity in an anteroposterior direction. According to histologic studies by Melsen,⁵ these sutures finish growth activity at 7 years of age (see Fig 2-1). The roof of the ethmoidal air cells (3) is not part of the frontal bone: The frontoethmoidal suture runs through the medial and lateral walls of the upper ethmoidal air cells. On lateral cephalograms, the cerebral surface of the roof of the ethmoidal air cells is usually easily visible (see Fig 2-2 [6]). The foramen rotundum (11) perforates the greater wing of the sphenoid, passing the maxillary nerve.

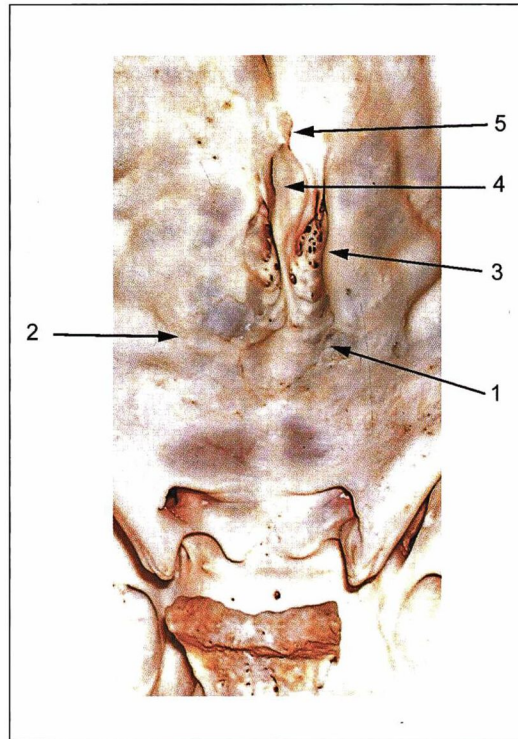


Fig 2-5 Internal surface (viewed from above) of the anterior cranial base in the skull of a child aged about 15 years (compare to Fig 2-4). 1. Remnants of the sphenothmoidal suture; 2. remnants of the frontosphenoidal suture; 3. roof of the ethmoidal air cells and ethmoidal crest; 4. crista galli; 5. foramen caecum. In the anterior cranial base, the sphenothmoidal suture (1) and frontoethmoidal suture (2) appear closed. The roof the ethmoidal air cells (3) is lateral and more superior than the cribriform plate, while the roof of the orbit is even higher and much more lateral. In the cephalogram (see Fig 2-2), all three structures can be seen: The lowest is the cribriform plate, the middle contour is formed by the roof of the ethmoidal air cells (3), and the most superior one is the roof of the orbit. The most superior ethmoidal air cells are partly projected between the cribriform plate and the image of the roof of the ethmoidal cells. Often their walls can be distinguished consistently in serial cephalograms and included in the tracing to enhance superimposition.

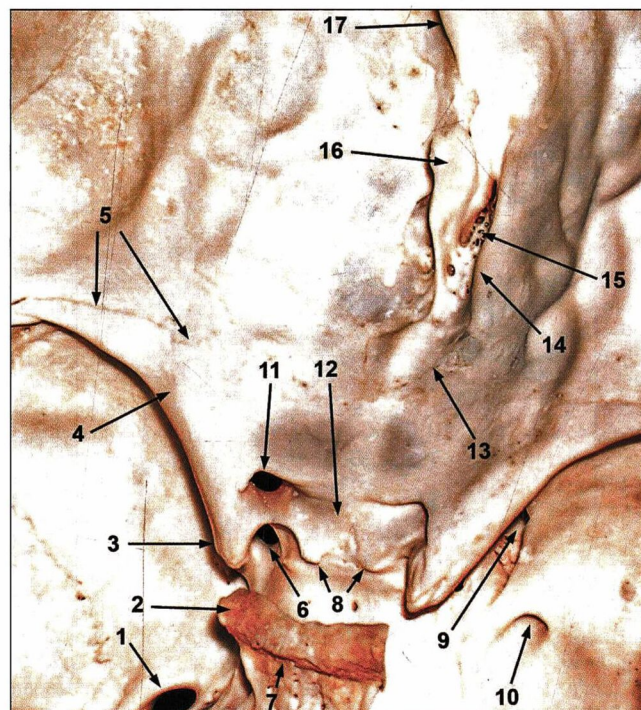


Fig 2-6 Internal surface (slightly oblique, viewed from above) of the anterior cranial base in the skull of a child aged about 15 years. 1. Foramen ovale; 2. posterior clinoid process; 3. anterior clinoid process; 4. posterior margin of the lesser wing of the sphenoid; 5. sphenofrontal suture; anterior margin of the lesser wing of the sphenoid; 6. superior orbital fissure (entrance); 7. dorsum sellae; 8. tuberculum sellae; 9. superior orbital fissure; 10. foramen rotundum; 11. optic canal; 12. sulcus chiasmatis (prechiasmatic groove); 13. sphenothmoidal suture; 14. roof of the ethmoidal air cells; 15. cribriform plate of ethmoid bone; 16. crista galli; 17. frontal crest of the frontal bone. The posterior clinoid process (2) and part of the dorsum sellae (7) were covered with cartilaginous tissue that was lost with the maceration process during specimen preparation. The sphenofrontal suture (5) and the sphenothmoidal suture (13) appear closed. These sutures are parts of the transverse coronal suture system together with the coronal, the sphenosquamosal, sphenozygomatic, and temporozygomatic sutures. The transverse sutural system allows for the sagittal forward growth of the anterior cranial fossae and midfacial bones. These sutures are not visible in cephalograms, but their location can be estimated (see Fig 2-7).

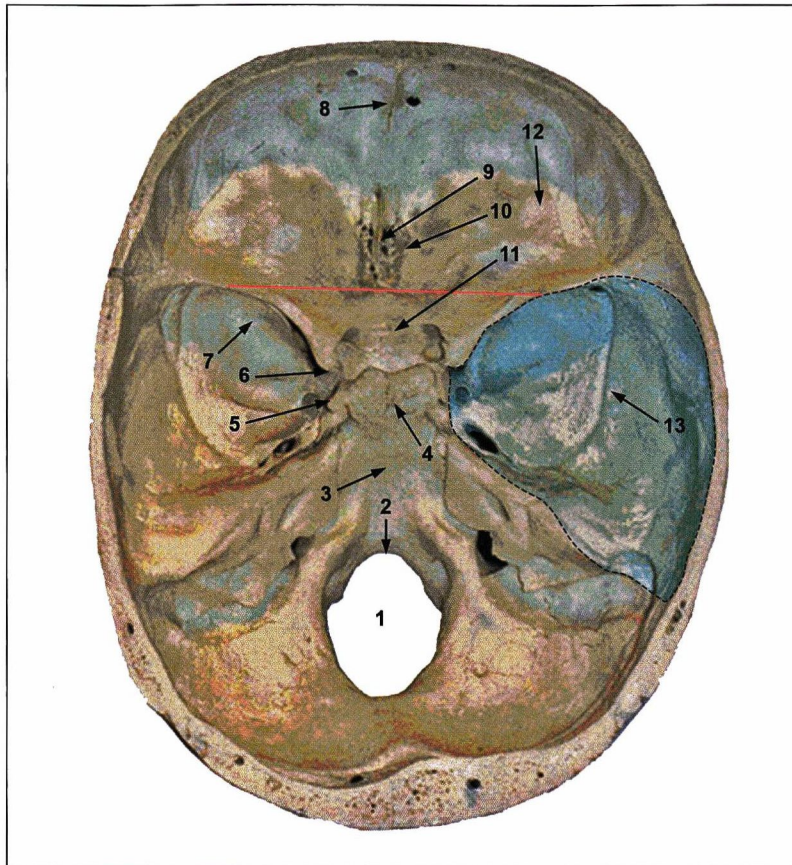


Fig 2-7 Internal surface (viewed from above) of the base of the adult skull. 1. Foramen magnum; 2. basion (midsagittal point at the anterior rim of the foramen magnum); 3. clivus; 4. dorsum sellae; 5. posterior clinoid process; 6. anterior clinoid process; 7. cerebral surface of the greater wing of the sphenoid bone; 8. frontal crest of the frontal bone; 9. cribriform plate; 10. roof of the ethmoidal air cells; 11. sulcus chiasmatis; 12. cerebral surface of the orbital part of the frontal bone; 13. middle cranial fossa (colored transparent blue). The red line touching the posterior borders of the lesser wings of the sphenoid bone crosses the midline approximately at the location of the sphenothmoidal suture. Variation has been found in the location and morphology of the sphenothmoidal and the sphenofrontal sutures.⁸ The cerebral surfaces of the greater wings of the sphenoid bone (7) are usually very visible in the cephalogram as double images. These surfaces form the anterior limits of the middle cranial fossae (see Fig 2-2 [9]). The middle cranial fossa (13) is limited by three structures: The anterior border is the greater wing of the sphenoid (7); the lateral border is the squamous part of the temporal bone; and the posterior border is the anterior surface of the petrosal part of the temporal bone. The frontal crest (8) is sometimes visible in cephalograms. However, the anterior limit of the anterior cranial fossa formed by the cerebral cortex (the inner table of the squamous part of the frontal bone) has better visibility (see Fig 2-2 [8]). Björk included this structure in tracings.⁹

(surface 3) and the sulcus chiasmatis (surface 4) show continued slow and even deposition of bone and reach stability only after puberty. Second, these areas are close to area 5, which makes this superimposition sensitive to rotational errors and/or incorrect horizontal and vertical registration. Figure 2-8 demonstrates the serious consequences of rotational errors.^{2,10}

Reliability of structural superimposition on the cranial base

With several different techniques possible in that time period, Houston and Lee¹⁰ reported on the accuracy of various procedures of superimposition on the cranial base using the Björk structural method. The authors warned that accuracy errors in superimposition give a misleading impression of facial growth. A 4-degree rotation of sella-nasion (S-Na) line, with S as the rotation point, gives rise to an appreciable displacement at the chin (see Fig 2-8).

Buschang et al¹¹ compared the technical reliability of structural superimposition on the cranial base and mandible as described by Björk and Skieller.⁹ Structural superimposition of the anterior cranial base was more reliable and required less training than local mandibular superimposition. The method errors for the cranial base superimposition ranged from 0.17 to 0.41 mm, while those for the mandible ranged from 0.37 to 0.93 mm. The vertical orientations on the posterior reference markers for both superimpositions show the greatest technical error. They concluded that the method is accurate and effective.

Since these studies were published, the general quality of cephalograms has improved. Also, currently available digital techniques allow for manipulation of radiographs in ways that may considerably enhance accuracy in individual cases. In addition to such improvements, techniques using individually prepared tracing templates further improve accuracy. Chapters 4, 7, and 8 describe these procedures.

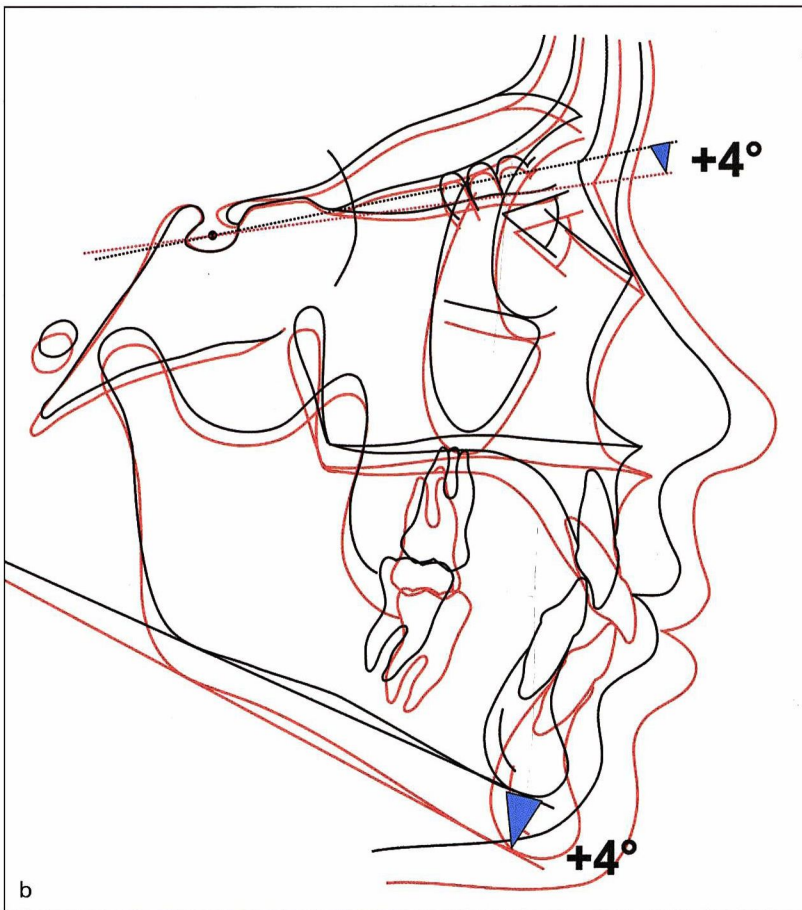
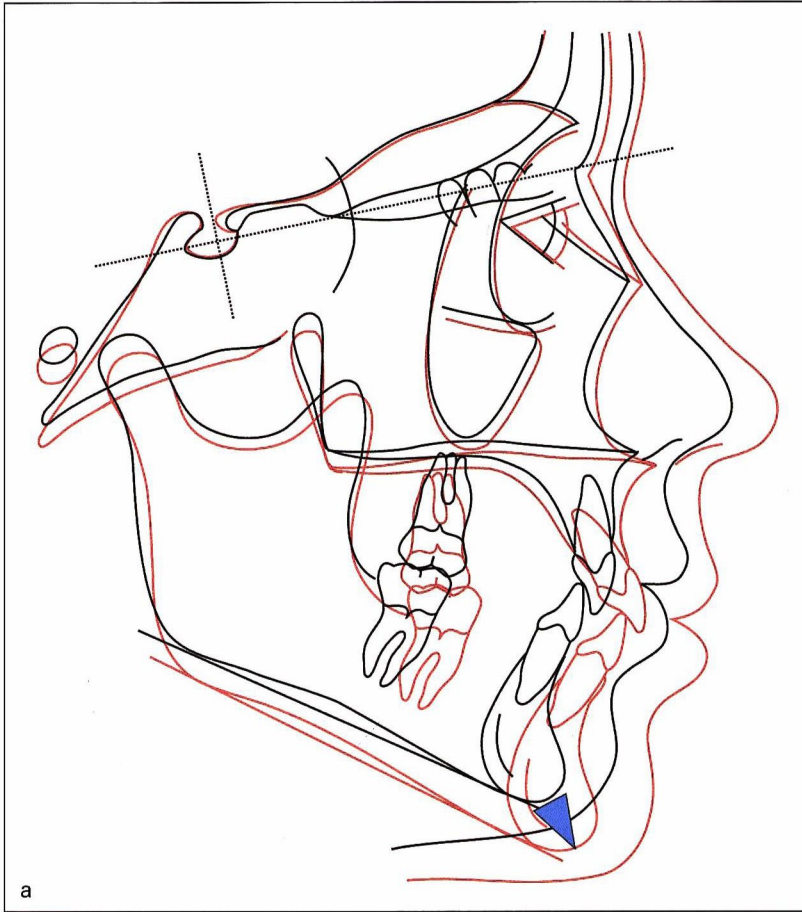


Fig 2-8 Effect of a small error in anterior cranial base superimposition. Compare the correct superimposition (*a*) to one showing a 4-degree rotation (*b*); identical tracings were used. The red tracing in *b* is erroneously superimposed, 1.2 mm too far downward, with the cribriform plate tracing, while in the anteroposterior direction the superimposition in the sella (S) region is correct. This leads to an erroneous 4-degree downward rotation with S as the center of the rotation (*small blue arrow*). The effect in displacements at the chin region, however, is considerable. It appears as if the anterior facial height increased considerably, the maxillary and mandibular region grew vertically downward, and the mandibular plane rotated 4 degrees more posteriorly than actually occurred with growth and treatment. Note the difference in direction of changes in the chin region (*large blue arrows*). Such errors may result in a misleading impression of facial growth. (Adapted from Houston and Lee¹⁰ with permission.)

Fig 2-9 Mandibular natural reference structures identified on cephalogram, as indicated by Björk and Skieller.⁹ 1. Outside cortical outline at the chin; 2. any trabecular structure in the lower part of the symphysis; 3. internal cortical outline of the symphysis; 4. fundus of the crypt of the molar from the time of mineralization of the crown until the start of root formation and also possibly of a premolar germ; 5. contours of the mandibular canal; 6. the contours of the anterior border of the ramus of the second tracing should be posterior, not anterior, to the first tracing. Björk and Skieller⁹ named this “the logical sequence of growth,” and it can be observed in Figs 2-10 and 2-11.

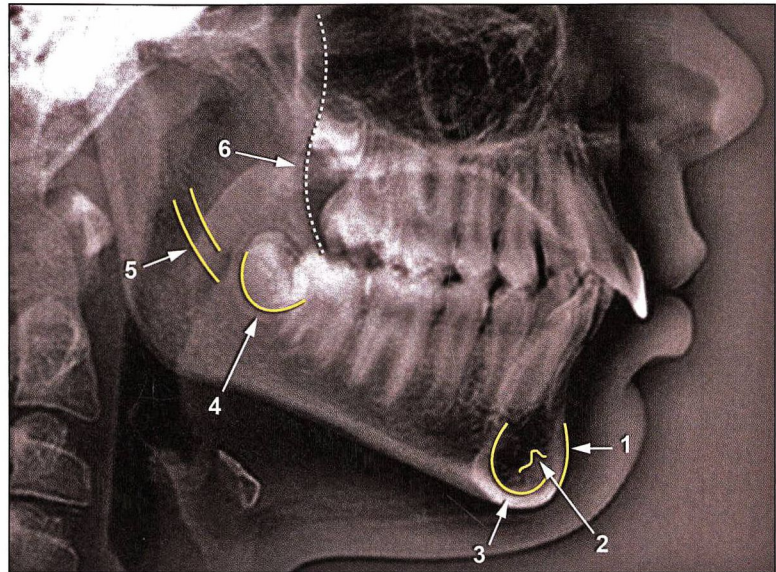
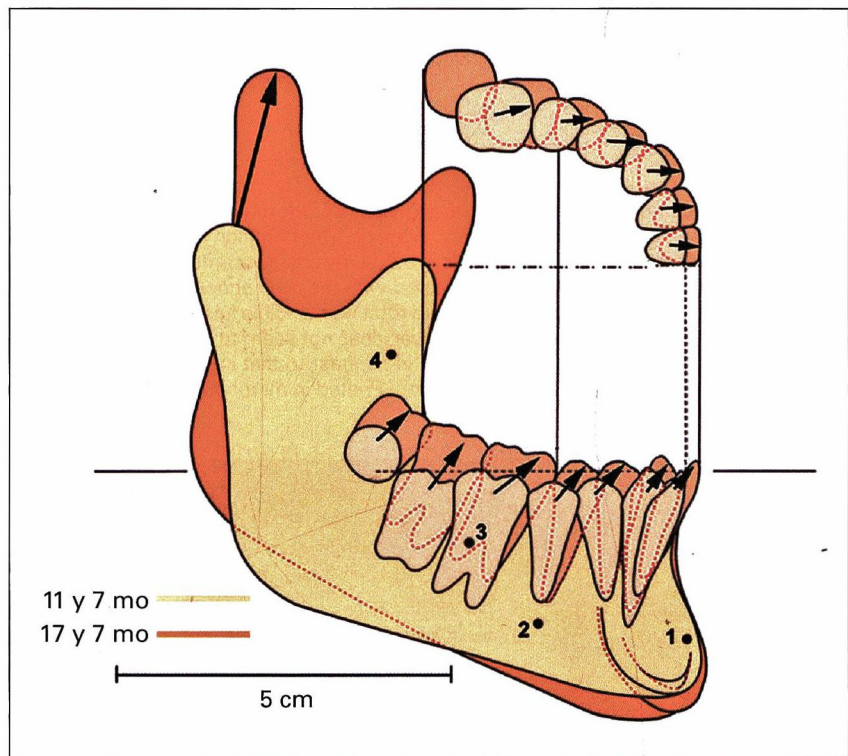


Fig 2-10 Superimposition on implants 1, 2, 3, and 4. In this example of extreme forward growth rotation, note the forward/upward-directed growth of the mandibular condyle and the forward/upward-directed drift of the complete dentition. Due to the forward rotation during growth, there appears to be no or little posteriorly directed drift of the anterior limit of the ramus, thus limiting space for the erupting permanent third molars. There was some endosteal resorption combined with considerable periosteal deposition at the most inferior region of the cortex of the symphysis. The fundi of the alveoli of the third molar and second premolar are superimposed. (Reprinted from Björk¹² with permission. Printed in mirror image, with color added by the authors.)



Method Error in Mandibular Structural Superimposition

Validity of mandibular structural superimposition

By superimposing radiographs on metallic implants in the mandible, Björk and Skieller⁹ detected bony areas in the mandible that appeared stable during determined periods

of time, which they labeled *natural reference markers*. Figure 2-9 shows the location of these markers (1 through 5). Marker 6, the anterior border of the ramus, plays a different role, as explained in the legend. In the paragraphs that follow, specific detailed attention is given to the evidence base for each of the five natural reference markers. Figures 2-10 and 2-11 are examples from Björk’s publications¹² demonstrating the results of implant studies and the use of natural reference markers. In 2010, Springate¹³ detected additional markers, and these are discussed as well.

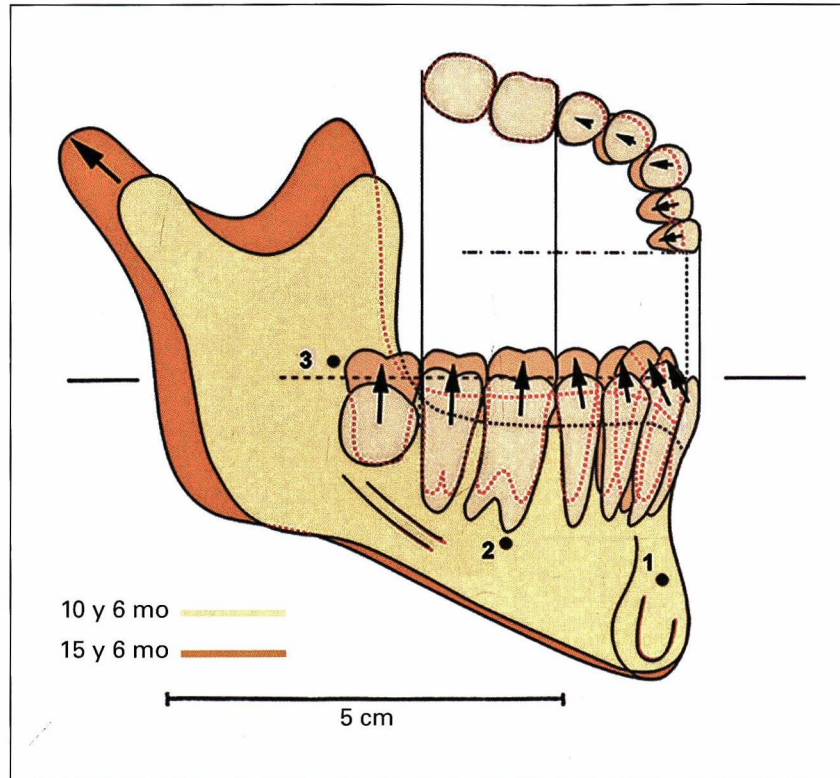


Fig 2-11 Superimposition on implants 1, 2, and 3. The growth of the condyle is in a posterior direction, and growth rotation is backward directed. The rate of condylar growth is approximately one-third the amount seen in the forward rotating mandible in Fig 2-10. The ramus is drifting in a posterior direction. The dentition drifts upward and, in the anterior region, even in a posterior direction. Space for third molar emergence is provided by posterior drift of the anterior contour of the ramus. The fundus of the alveolus of the third molar is superimposed. Compared with the case shown in Fig 2-10, only a small amount of bone is deposited under the chin (about 0.6 mm per year in the forward rotating mandible and approximately 0.2 mm in the backward rotating mandible). The vertical growth of the alveolar process, however, does not seem to be much different. The endosteal surface in the symphysis has remained stable during the observation period, in contrast to that in the forward rotating mandible, in which some resorption has occurred. (Reprinted from Björk¹² with permission. Printed in mirror image, with color added by the authors.)

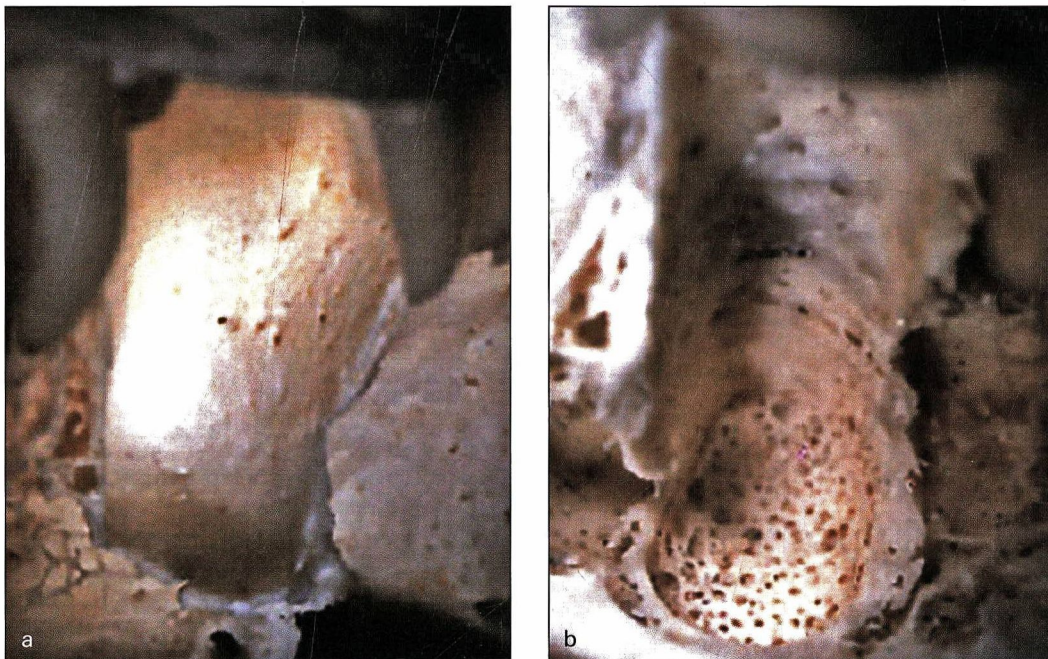


Fig 2-12 (a) Fundus of the crypt of a premolar before active deposition takes place. (b) Rapid bone deposition took place in the fundus of the crypt of this premolar. The rapid eruptive movement of the tooth occurs during this stage, and remnants of the original fundus can still be seen. They are sometimes also visible on radiographs and can then still be used as a reference structure.¹⁴ (Reprinted from van der Linden and Duterloo¹⁵ with permission.)

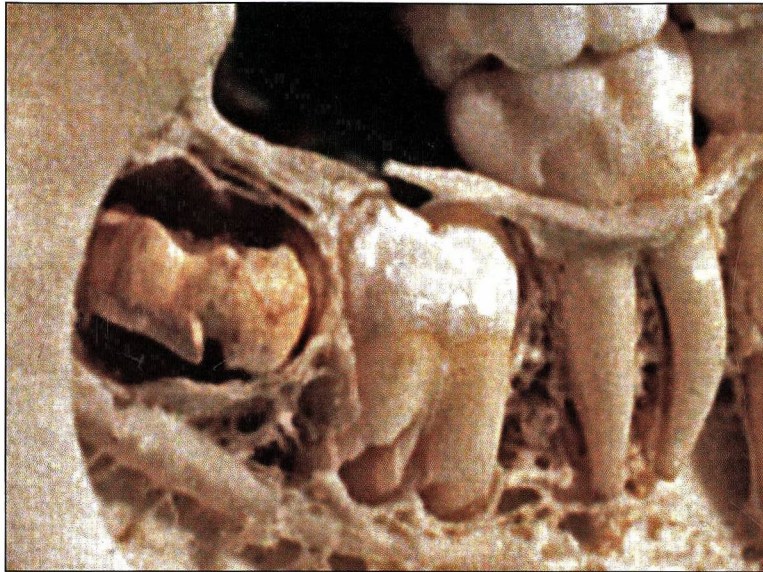


Fig 2-13 Details of the internal morphology of the mandible of a child of approximately 10 years of age. Note the close relationship of the fundus of the crypt of the mandibular right third molar and the roots of the mandibular right second molar to the mandibular canal. The internal surfaces of the crypt fundi of the second and third molars are smooth, indicating resting surfaces or very slow bone deposition. The position of the partly developed crown of the third molar has changed postmortem.

Remodeling of dental crypts

Evidence to validate these natural reference markers comes from histologic studies of the remodeling of dental crypts of unerupted molars in the mandible (and maxilla). It was shown that the fundus of the dental crypt is stable from the start of crown calcification during root formation until the start of the rapid eruptive movement of the tooth (Fig 2-12). In that period, the crypt fundus can be seen clearly and used for superimposition.¹⁴⁻¹⁸ In exceptional circumstances, when the eruption movement is hindered, the root apex may grow downward for some time.¹⁴

In clinical applications the third molar crypt is of limited use as marker because of its large developmental variation and the relatively short time frame.

Mandibular canal

Histologic evidence to support the use of the wall and/or the trabecular pattern around the most dorsal part of the mandibular canal (see Fig 2-9, marker 5) is not immediately apparent. In all likelihood, in the lateral view, bone remodeling around the canal is slow, follows the dorsolateral drifting of the ascending ramus and the lengthening of the neurovascular bundle, and maintain a relative spatial position. Occasionally, the persistence of trabeculae related to the canal can be seen in serial lateral cephalograms. Figure 2-13 shows the close spatial relationship between the crypt fundus and the canal in childhood.

Krarup et al¹⁹ performed a three-dimensional (3D) analysis of mandibular growth (Fig 2-14). The materials of the study consisted of the records of 10 children with Apert syndrome (5 boys and 5 girls). The mandible in such cases is normal in size and shape. All patients received craniofacial computed tomography scans in connection with diagnosis, treatment planning, and postoperative follow-up. Structural superimposition was performed according Björk and Skieller⁹ for conventional lateral cephalograms. The results supported the relative stability of the mandibular canal in the lateral view, as proposed by Björk and Skieller⁹ in 1983. However, the mandibular canals increase in length and are actually relocated laterally. Moorrees et al⁴ stressed the importance of the location of a natural reference marker in the distal portion of the mandible because this is the area where most growth occurs.

The canal is imaged as an upward curve in the gonial area, where its horizontal path changes vertically toward the mandibular foramen and the lingula. The part of the canal dorsal of the permanent first molars forms during postnatal growth, and its curvature relates to the ramal growth pattern.²⁰ Only occasionally, the full length of the bony cortex around the neurovascular bundle is seen. The visibility of the canal appears related to the cancellous bone density.²¹ The recent study by Springate¹³ confirms the stability in lateral view, particularly of the anterior part of the canal. Double images are normal. Occasionally the panoramic view is helpful for identifying structures (Fig 2-15). Thus, it appears logical to use the part of the image of the canal that is closest to the first molar.

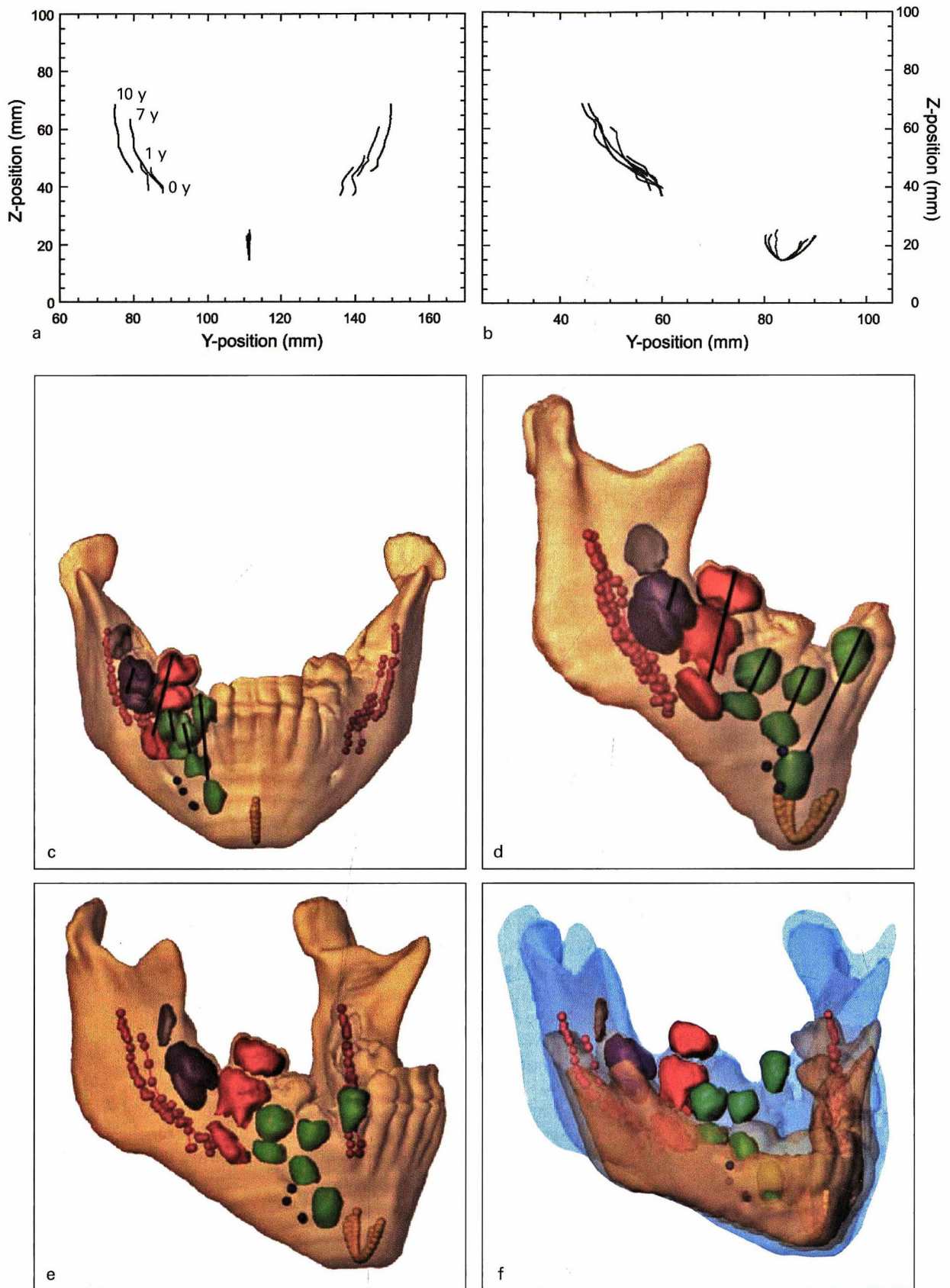


Fig 2-14 Records from the same individual from the study by Krarup et al¹⁹ at four different ages: 0, 1, 7 and 10 years. *Color code:* gray = permanent third molar; purple = permanent second molar; red = permanent first molar; green = permanent premolars and canines; blue = mental foramen; yellow = symphysis menti; pink = mandibular canals. (a) Superimposed computed plots of the frontal view, showing the symphysis menti and the mandibular canals. Note the lateral movement of the mandibular canals. (b) Superimposed computed plots of the lateral view, showing the symphysis and the mandibular canals. Note the relative stability of the curvature of the mandibular canals in this lateral view. (c) Frontal view of the mandible at age 10 years. Mental foramina and segmented teeth (posterior to the incisors) from four different ages (0, 1, 7, and 10 years) are automatically aligned on the symphysis menti and the mandibular canals. Only the teeth and the mental foramina on the right side are illustrated. Lines indicate the eruption paths of the individual teeth. (d) Lateral view. Lines indicate the eruption paths of the individual teeth. (e) Oblique view. (f) Three-dimensional superimposition of transparent mandibles at four different ages (0, 1, 7, and 10 years). Mental foramina and segmented teeth (posterior to the incisors) are automatically shown with superimposition on the symphysis and the mandibular canals. Only the teeth and the mental foramina on the right side are illustrated. (Adapted from Krarup et al¹⁹ with permission.)